

# OIL SPILLS FROM THE DOUBLE HULL MODEL TANKS\*

By

Katsuji YAMAGUCHI\*\*

Hiroshi YAMANOUCHI\*\*

## Abstract

Cargo behaviors of double hull tankers after groundings and collisions which result in the rupture of both the outer hull plating and the inner hull plating were investigated using the 1/50 scale models representing a mid-ship section of a typical cargo tank of VLCC. Tests were carried out in still water, and a lubricating oil was used as the test fluid. Oil outflows were measured under the various conditions for the double bottom heights and the double side widths, the tank sizes, the extent and the position of the rupture, the axial offsets of the ruptures, the initial thickness of the water layer in the double hull space, the drafts and the cargo levels.

The dynamic characteristics of water and cargo flow in the double hull space after an opening of the rupture were examined.

An analysis was presented for the amount of oil outflow from the ruptured ship tank model with double hull.

---

\* Received on May 5, 1992

\*\* Ship Equipment and Marine Environment Division

## TABLE OF CONTENTS

1. INTRODUCTION
2. EXPERIMENTAL APPARATUS
3. MODEL TANK
4. EXPERIMENTAL PROCEDURES
5. TEST PARAMETERS AND TEST CONDITIONS
6. OBSERVATIONS OF OIL SPILLS
  - 6.1 Bottom rupture
  - 6.2 Side rupture, below water line
  - 6.3 Side rupture, on water line
7. RESULTS
  - 7.1. Quantity of oil outflow
    - 7.1.1. Bottom rupture
    - 7.1.2. Side rupture, below water line
    - 7.1.3. Side rupture, on water line
8. ANALYSIS OF RESULTS
  - 8.1 Oil outflow
  - 8.2. Non-dimensional thickness of water layer  $\alpha$
  - 8.3. Quantity of oil contained in double hull space
  - 8.4. Oil spill fraction
9. CONCLUSIONS
  - NOMENCLATURE
  - ACKNOWLEDGEMENTS
  - APPENDIX

## 1. INTRODUCTION

Recent environmental pollution in the sea and on the beaches resulting from oil spills from tanker has become the object of public attention to improving the tanker design to avoid oil spills in accidents. Double hull ships are accepted in 1992 by the International Maritime Organization (IMO) as one of new future ships for minimizing oil spills in the event of a casualty. Consequently, several publications dealing with the design of double hull tanker have appeared in the literature. However, data in understanding fundamental physical processes involved and data of oil spills from a ship with double hull during the accident are limited, consequently, published analyses for estimating oil spills in particular accident scenarios are based on simplified assumptions. More basic knowledge is required to develop the sufficiently accurate and reliable computation models for predicting oil outflow from a damaged ship with double hull.

The purpose of this paper is to provide data to evaluate quantitatively the performance of the double hull tanker design in reducing environmental oil pollution in the collision and grounding accidents. So, tests of oil spills from the model tank were conducted in still water for a variety of accident scenarios, cargo and tank conditions. The effects of the tidal current, the waves, the heel, and change in draft during the accidents on oil spills were not discussed in this paper. Model geometry and model dimensions were determined from typical double hull ship data.

## 2. EXPERIMENTAL APPARATUS

The schematic diagram of the experimental apparatus is shown in Fig.1.

The experimental apparatus consists of a double hull model tank which was hold vertically to a supporting frame so as to eliminate movement, a water basin with sight glass, oil pumps to recover oil spilled from the model tank, a oil-water separator, water feed line to supply water to the water basin and to keep preselected water level during the tests, oil feed line to supply oil to the model tank and a vacuum pump to evacuate water and/or oil from the double hull space of the model tank. The dimensions of the water basin are 5.0 m in length, 0.8 m in breadth, and 1.0 m in depth.

## 3. MODEL TANK

The tests were conducted with an open double hull model tank shown in Fig.2 having height of 0.6 m, breadth of 1.2 m, and length of 0.45 m. The wall thickness of the model tank made of stainless steel is 4 mm. The inner tank, that is the oil cargo tank, is smaller than the outer tank by the double bottom height and the double side width. Double bottom is divided breadthwise into two parts at the center and forms the J tank configuration.

Reinforcement members were bolted in the double hull space to increase the stiffness of the model tank. Flows of oil and water within the double hull are not disturbed significantly and are not prevented by the members.

The front and rear of the model were constructed of Plexiglass (thickness of 13 mm) in order to make visual observations.

The model tank is the 1/50 scale model of a typical cargo tank section of VLCC with simplified middle part. The dimensions of the model tanks are summarized in Table 1.

Three sizes of the model were made. The configuration of the models represents the geometries designed in many practical applications. The double bottom height and the double side width are same and are 20 mm, 40 mm and 60 mm in sizes respectively.

For use of the models in testing oil spills in the events of the groundings and collisions damages, the smooth-edge circular punctures were drilled into the tank bottom walls and into the tank side walls. The

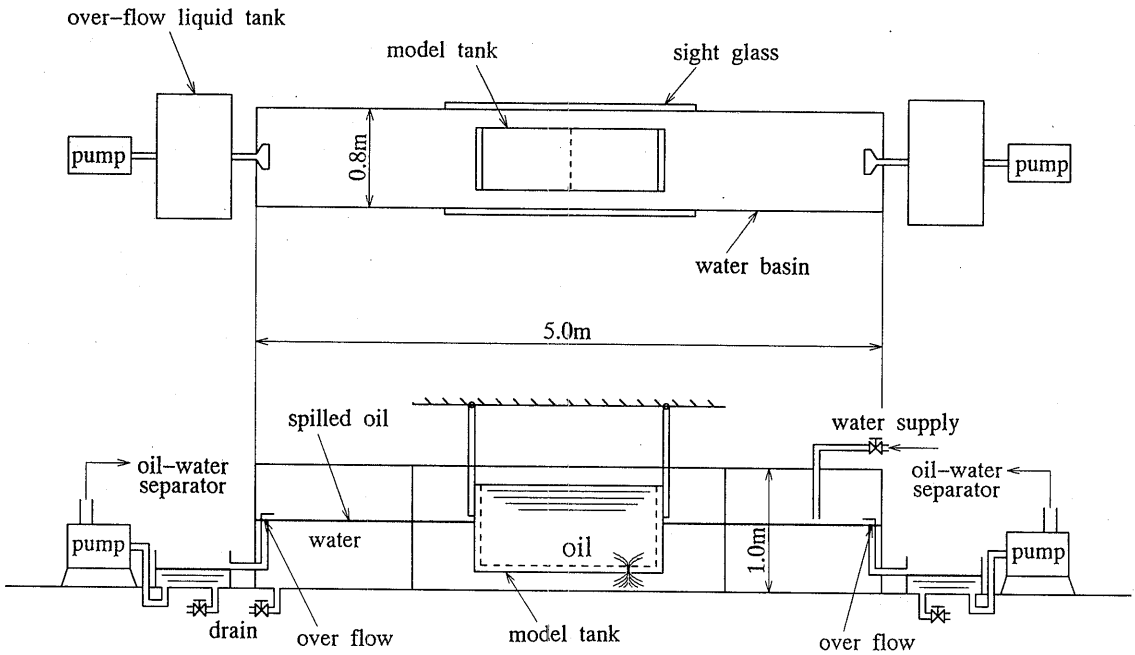


Fig. 1 Schematic diagram of experimental apparatus

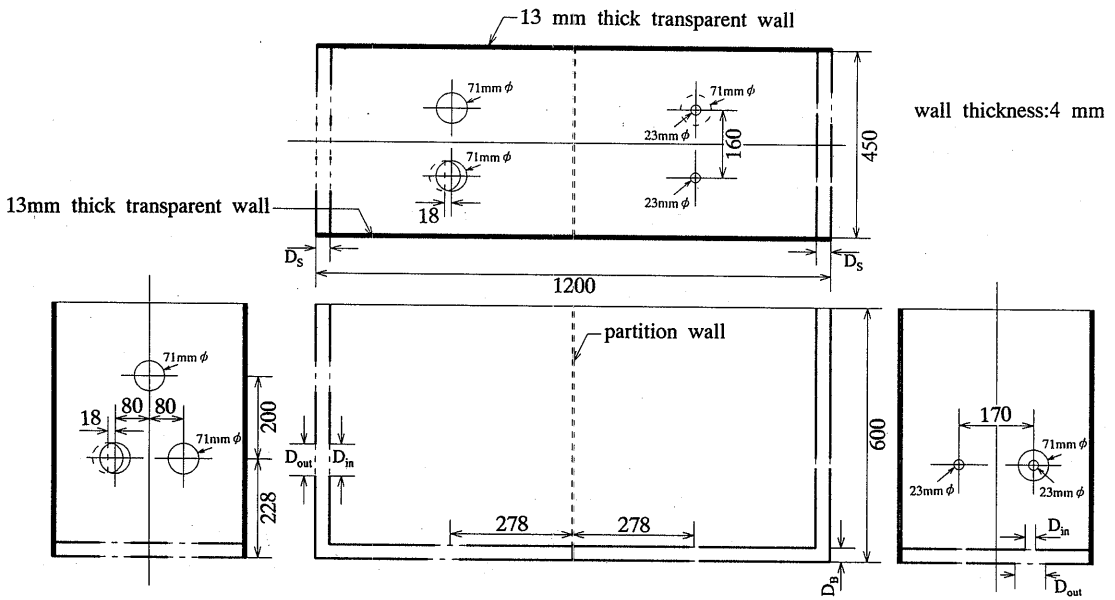
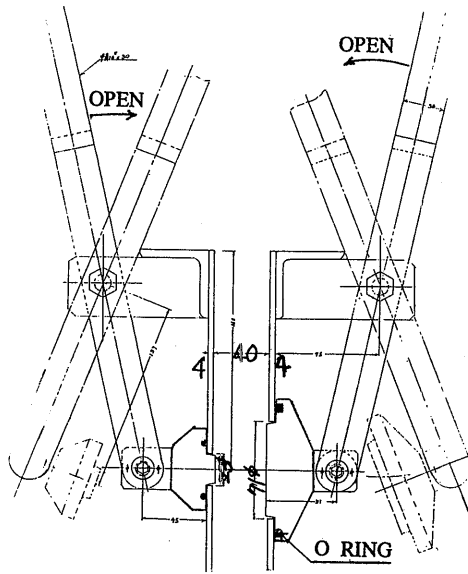
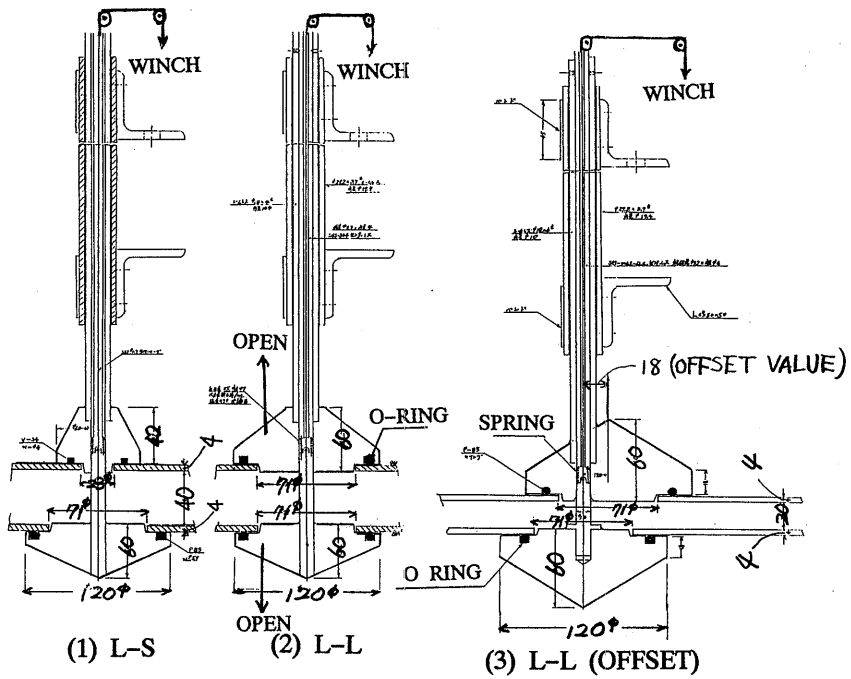


Fig. 2 Model tank



OPENINGS (TANK SIDE  
LARGE-SMALL)



OPENINGS (TANK BOTTOM)

Fig. 3 Details of rupture plugs

Table 1 Dimensions of model tank

Model	Breadth	Depth	Side Width	Double bottom Height	Length
M1	1200 mm	600 mm	20 mm	20 mm	450 mm
M2	1200 mm	600 mm	40 mm	40 mm	450 mm
M3	1200 mm	600 mm	60 mm	60 mm	450 mm

simulated punctures were attached coaxially or with an offset to the inner plating and outer plating of the model tank as shown in Fig.2. The smaller punctures were 23 mm in diameter, and the larger ones were 71 mm both for the outer shell and the inner shell plating. The combinations of the puncture sizes of outer plating and inner plating are large-large, small-small and large-small for the coaxial case and large-large for the case with an offset value of  $0.25 D_0$ .

The inner plating puncture and the outer plating puncture were sealed tightly with plugs. In the tank bottom case, they were opened simultaneously by pulling the inner plating plug inward and by releasing a suspended outer plating plug by means of a wire of 1 mm in diameter. In the tank side case, inner plating plug and outer plating plug were opened simultaneously by lever. The detail of the plugs are shown in Fig.3. The lift of the plug of inner hull puncture is approximately 50 mm.

#### 4. EXPERIMENTAL PROCEDURES

For a given test, the cargo oil tank of the model tank was filled with the test oil to a preselected level. The model is supported in the water basin rigidly and vertically by frame structure at desired water level. The oil and water in the double hull are carefully removed before the experiments by the vacuum pump with specially designed intake nozzle. The water level in the water basin was adjusted by supplying the tap water or pumping out water. By opening the punctures quickly and simultaneously, the cargo oil flows out to the double hull space and into surrounding water. Surrounding water flows into the double hull space. After certain time later, the oil outflow from the model tank and water inflow to the tank come to an end. All tests are recorded with the video tape recorders through the video cameras. Change of the oil level in the cargo tank before and after the experiment, oil and mean water level in the double hull space were measured visually to calculate the oil outflow from the cargo oil tank, oil and water inflow to the double hull space and the oil outflow from the tank.

#### 5. TEST PARAMETERS AND TEST CONDITIONS

Experimental conditions and variables employed have to correspond to the actual conditions. Tests were conducted for simplified and typical conditions due to extreme complexity of real situations. Data obtained from these conditions serve as a baseline with which to understand the more realistic conditions.

A lubricating oil was selected as the test fluid since the density of the oil is near that of the typical crude oil. Also this oil is easy to handle. The density was  $860 \text{ kg/m}^3$  at  $15^\circ\text{C}$  and the viscosity was  $31.4\text{cSt}$  at  $40^\circ\text{C}$ .

The parameters are as follows:

- 1) tank geometry
  - double bottom height
  - double side width
  - cargo oil tank (no-dividing, dividing)
  - double bottom configuration (J type)
- 2) accident scenario
  - grounding (rupture location: on tank bottom)
  - collision (rupture location: on tank side)
  - rupture position (coaxial, offset)
  - rupture size (large-large, small-small, large-small)
  - thickness of water layer in double hull space
- 3) condition of shipment
  - initial cargo oil level (measured from inner bottom plating)
  - draft (measured from outer bottom plating)

The ranges of variable are summarized in Table 2 and Fig.4 shows the notations. The rupture of the inner hull plating will be initiated later than that of the outer hull plating in some accident scenarios. In this case, surrounding water flows into the double hull space and forms the water layer before the initiation of oil discharge from the oil tank. Difference in the rupture initiation time between the hull platings is simulated by the initial thickness of the water layer in the double hull space. Temperature of test fluids was  $15 \pm 4^\circ\text{C}$ .

Table2 Experimental conditions investigated

1) rupture location: tank bottom

$D_B/D_S$ (m)	$S_{o_2}$ (m <sup>2</sup> )	$D_o-D_i$	$\Delta$ (mm)	$t_i$ (mm)	$H_1$ (mm)	$d$ (mm)
0.02	0.52	L-L	0	0	200-500	200-460
				96-396	500	200, 400
0.04	0.5	L-L	0	0	300-500	200-450
	0.26	L-L	0	0	300-500	200-450
				10-38	500	300
		S-S	0	0	350-500	200-450
0.236	L-L	18	0	350-500	200-450	
0.06	0.48	L-L	0	0	300-500	200-450
				10-55	500	450
		S-S	0	0	300-500	200-450
	L-S	0	0	300-500	200-450	

$$D_B/D_o = 0.28-2.6$$

$$A_o/S_o = 0.0008-0.015$$

$$V_D/V_o = 0.04-0.17$$

$$d/H_1 = 0.4-1.0$$

2) rupture location: tank side

$D_B=D_S$ (m)	$S_{o_2}$ (m <sup>2</sup> )	$D_o-D_i$	$\Delta$ (mm)	rupture location
0.04	0.5	L-L	0	below water line
	0.26	L-L	0	on water line
0.06	0.48	L-L	0	below water line

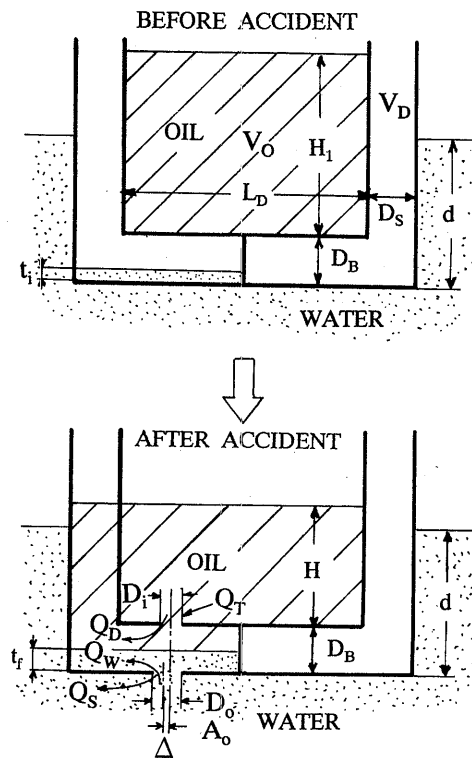


Fig. 4 Notations, and cargo oil before accident and after accident



## 6. OBSERVATIONS OF OIL SPILLS

All tests were observed and recorded by video tape recorders. Several test recordings were printed by video printer. Main feature of oil spill behaviors will be described for every rupture location.

### 6.1. Bottom rupture

With opening both the ruptures of inner bottom plating and outer bottom plating simultaneously, water flows into the double hull space against the opposing oil outflow, then two opposing streams impact. The impact position is moved toward the outer plating rupture from the first instant of impact. The oil begins to spill from the outer hull when the impact interface is reached to outside the tank. During oil spill, part of leaving oil from oil tank flows into the double hull space, admitting water inflow. If the hydrostatic head of water is sufficiently higher than the head of oil, oil spill will not occur. Water-oil interface will move far from tank wall depending on the velocity of oil outflow.

As the oil level in the oil tank falls, outflow velocity decreases and water-oil interface approaches to the tank bottom wall, finally it reaches to the outer shell plating. The net pressure difference across the rupture becomes zero, and the water inflow and oil outflow will cease.

Photo.1 shows time history of the test of violent oil outflow and small amount of water inflow into the double bottom after the ruptures opened. Photo.2 shows the test of small amount of oil outflow and large amount of water inflow into the double bottom. Left row is a whole view and right row shows a detail flow behaviors near the ruptures.

Photo.3 shows the oil spill flow when water is introduced into the double bottom before the test. With opening the ruptures, oil is discharged into both the surrounding water and the double bottom. Introduced initial water flows out through the rupture. Remaining water rises the double side space. After violent oil outflow is completed, water in side space is displaced by oil until filled with oil. The thickness of the water layer gradually decreases with increasing the oil thickness due to pushing out from the rupture to the environment by oil.

### 6.2. Side rupture, below water line

With opening the ruptures, oil outflow begins. Oil and water flow into the double hull space. As the oil level in the oil tank decreases, the outflow velocity decreases. The liquid level in the double side space is above the puncture. When oil tank level, liquid level in the double hull space and surround water level are all of equal height, displacement of oil by water both in oil tank and in the double hull space will be started. Once started, displacement will continue until the top of the puncture becomes equal to the oil-water interface in both oil tank and side space. Consequently, additional cargo oil will be spilled by water-oil displacement after the net pressure difference across the rupture becomes zero. Photo.4 shows the time history of oil outflow and water inflow for the double bottom height of 0.04 m.

### 6.3. Side rupture, on water line

At the beginning, oil is discharged at high rate owing to the high hydrostatic head of oil, admitting water and oil inflow to the double hull space. Decreasing the hydrostatic head of oil decreases the outflow velocity, and increases the oil and water inflow to the double hull space. Approaching the oil tank level to the draft and to the liquid level in the double hull space, then the oil in the oil tank and in the double hull space begins to displace. Additional oil starts to spill. All amount of oil will be spilled. Cargo oil tank and the double hull space are filled with water. Photo.5 shows the time history of the whole cargo oil is spilled.

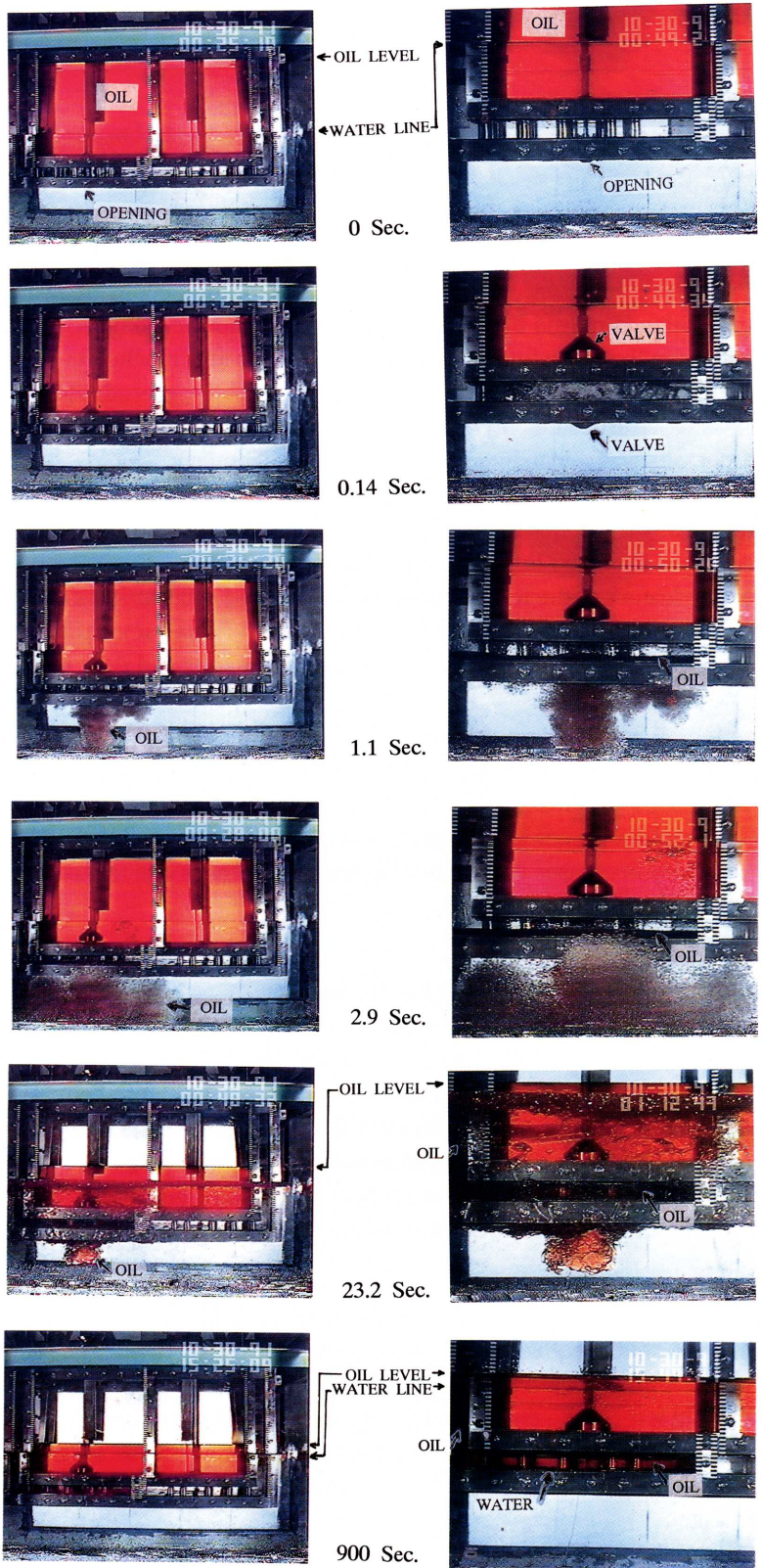


Photo.1 Huge oil spills from bottom rupture  
 $(H_1=0.5 \text{ m}, d=0.2 \text{ m}, D_B=D_S=0.04 \text{ m},$   
 $D_o=D_i=71 \text{ mm}\phi)$

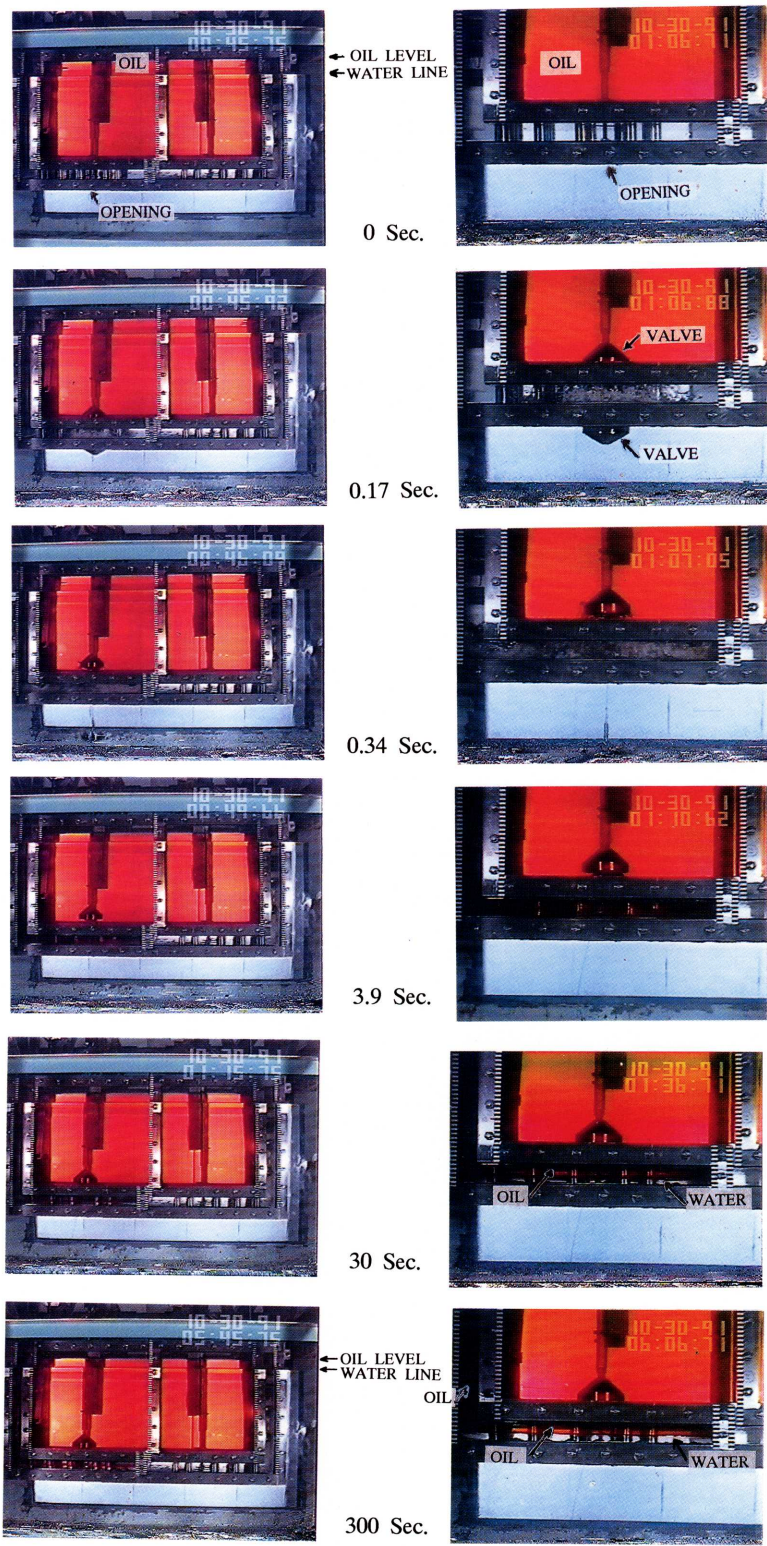


Photo.2 Tiny oil spills from bottom rupture  
 $(H_1=0.5 \text{ m}, d=0.45 \text{ m}, D_B=D_S=0.04 \text{ m},$   
 $D_o=D_i=71 \text{ mm}\phi)$

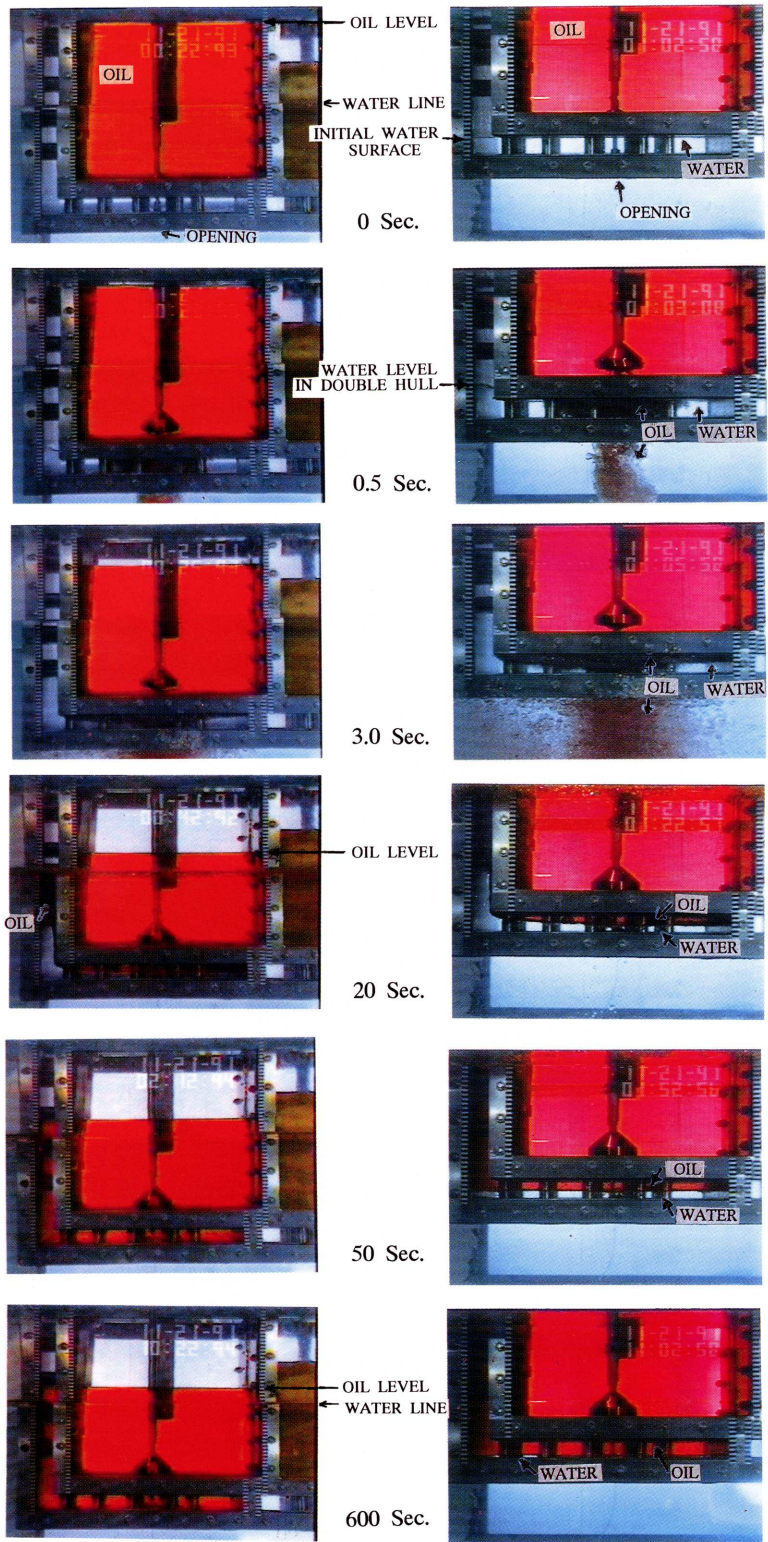


Photo.3 Oil spills through water layer  
 ( $t_i=38$  mm  $H_i=0.5$  m,  $d=0.3$  m,  $D_B=D_S=0.04$  m,  
 $D_o=D_i=71$  mm $\phi$ , opening: bottom)

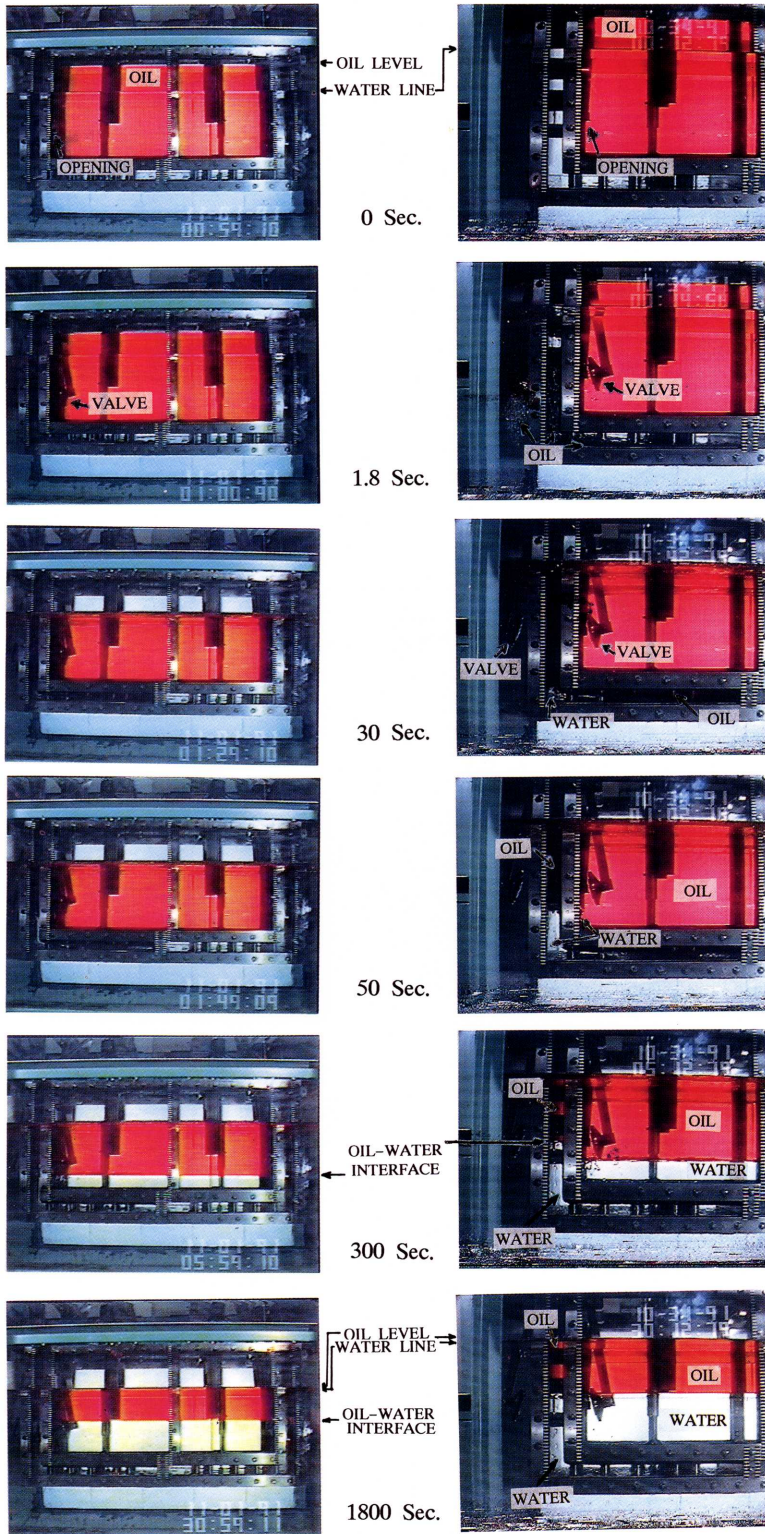


Photo.4 Oil spills from side rupture, below water line  
 $(H_i=0.48\text{ m}, d=0.38\text{ m}, D_B=D_S=0.04\text{ m},$   
 $D_o=D_i=71\text{ mm}\phi)$

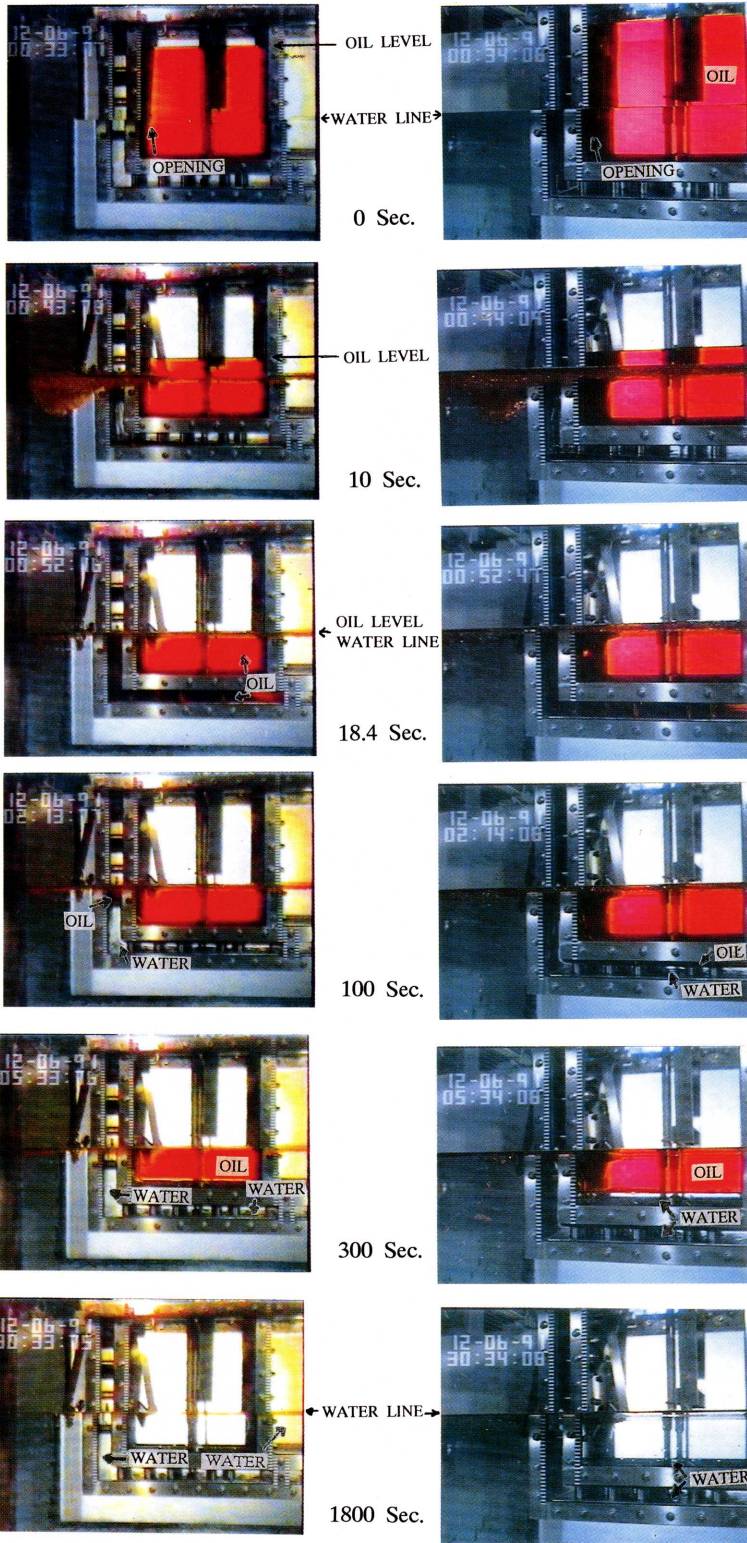


Photo.5 Oil spills from side rupture, on water line  
 $(D_B=D_S=0.04\text{ m}, D_o=D_i=71\text{ mm}\phi)$

7. RESULTS

7.1. Quantity of oil outflow

7.1.1. Bottom rupture

1) Effect of liquid level on oil spills

Figs. 5, 6 and 7 show a plot of quantities of oil leaving from oil tank  $Q_T$  ( $m^3$ ), oil outflow from tank  $Q_S$  ( $m^3$ ), oil inflow to double hull space  $Q_D$  ( $m^3$ ) and water inflow to double hull space  $Q_W$  ( $m^3$ ) versus draft  $d$  measured from outer surface of outer hull plating for double bottom height of 0.02 m. The initial oil level measured from the inner surface of inner hull plating  $H_1$  was taken as parameter.

In these figures, the curves for various oil levels are seen to show similar tendency. When the difference between  $H_1$  and  $d$  is large,  $Q_T$  and  $Q_S$  are large. As the difference decreases, the values of  $Q_T$  and  $Q_S$  decrease. The variations of  $Q_D$  and  $Q_W$  for  $d$  are small, however, as the difference between  $H_1$  and  $d$  decreases,  $Q_D$  and  $Q_W$  change sharply.

Figs. 8, 9 and 10 show a plot of  $Q_T$ ,  $Q_S$ ,  $Q_D$ , and  $Q_W$  versus  $H_1$  for taking  $d$  as parameter. The curves expressing the relation between volume  $Q$ ,  $H_1$  and  $d$  show similar tendency as shown in figs 5 to 7.

Figs. 11 and 12 show oil spill data for double bottom height of 0.06 m showing that the tendency of oil spill does not change much for a variation of double bottom height.

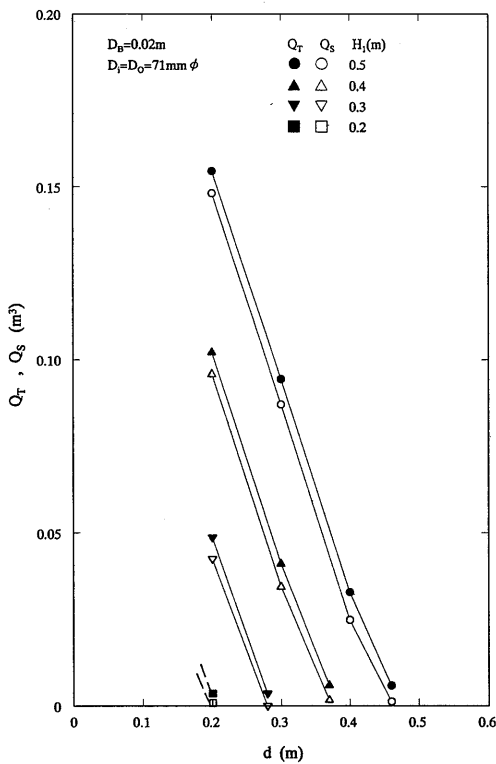


Fig. 5 Quantities of oil spills and oil leaving from oil tank (parameter:  $H_1$ )

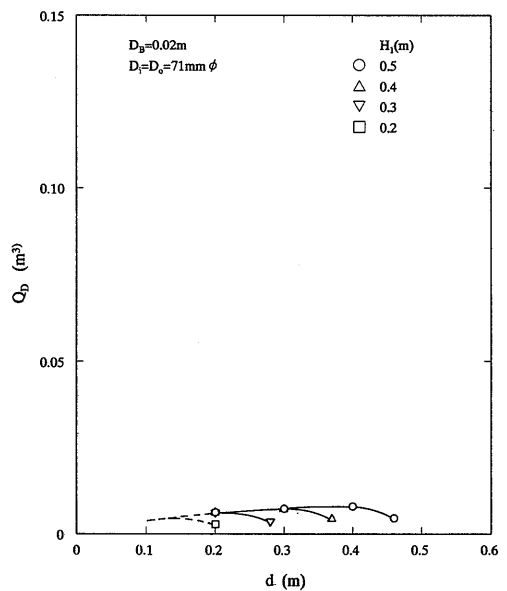


Fig. 6 Quantity of oil containment in double hull space (parameter:  $H_1$ )

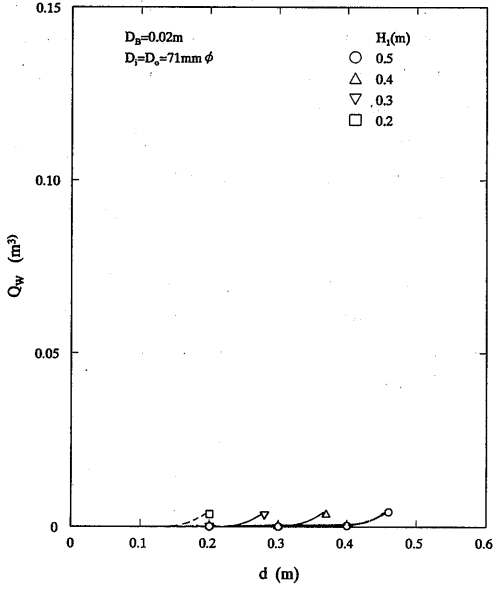


Fig. 7 Quantity of water flows into double hull space (parameter:  $H_1$ )

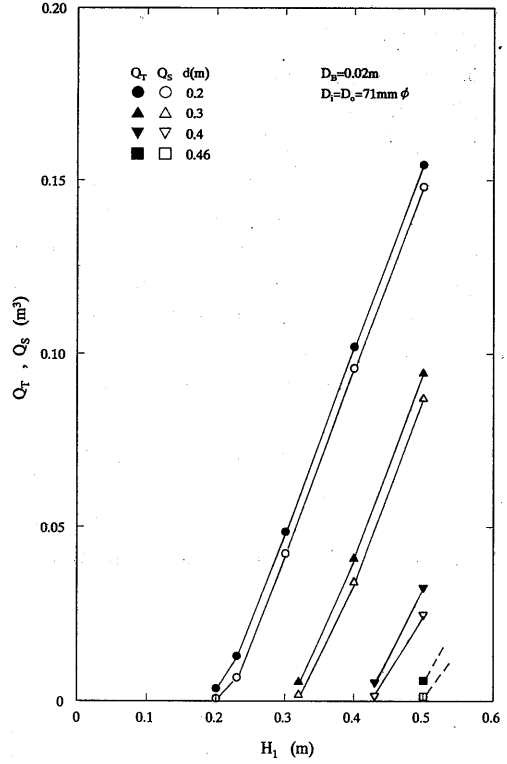


Fig. 8 Quantities of oil spills and oil leaving from oil tank (parameter:  $d$ )

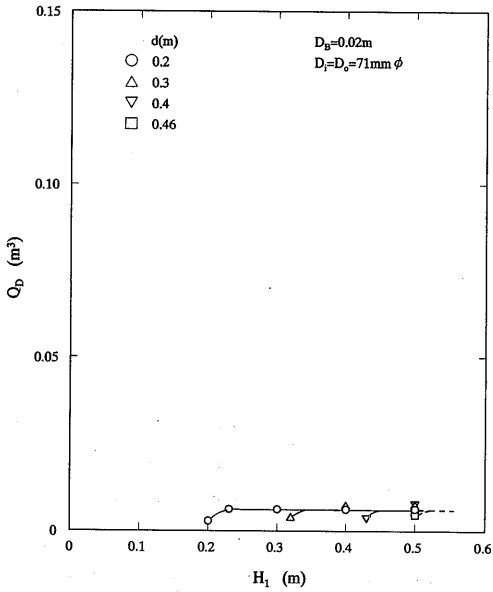


Fig. 9 Quantity of oil containment in double hull space (parameter:  $d$ )

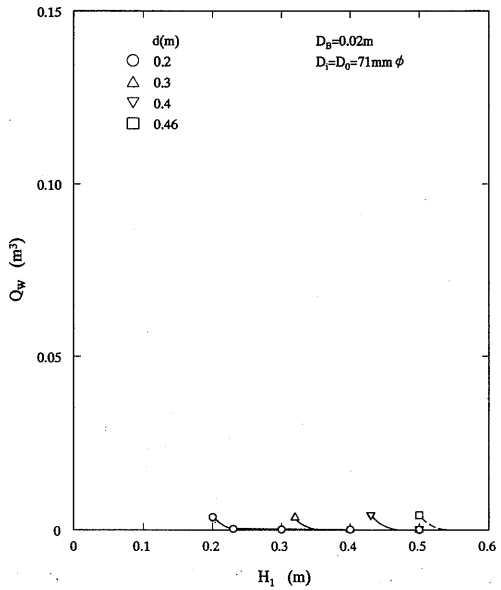


Fig. 10 Quantity of water flows into double hull space (parameter:  $d$ )



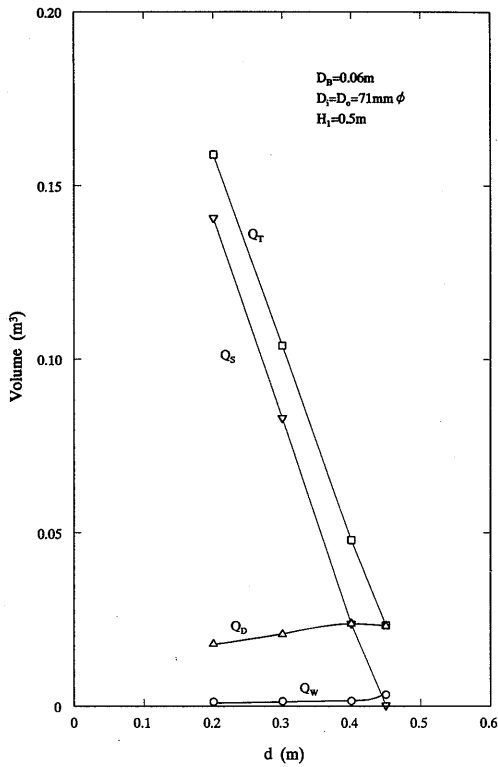


Fig. 11 Quantity of oil outflow and water inflow ( $H_1=0.5$  m)

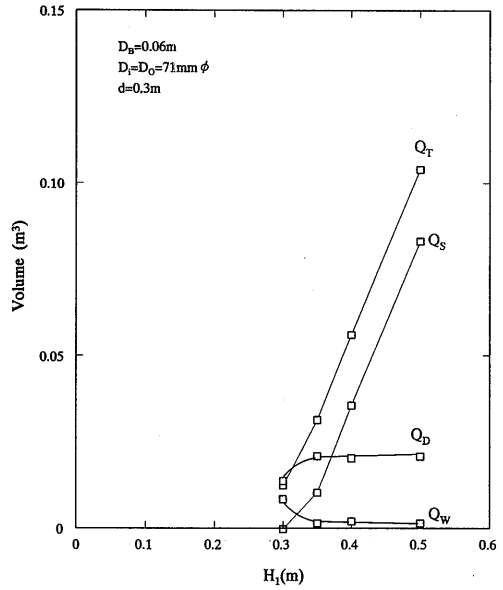


Fig. 12 Quantity of oil outflow and water inflow ( $d=0.3$  m)

2) Effect of cross-sectional area of oil tank

The effect of cross-section area of oil tank  $S_0$  ( $m^2$ ) on  $Q_T$ ,  $Q_S$ ,  $Q_D$ , and  $Q_W$  was investigated by using the oil tank of one and two divisions. The curves for different  $S_0$  in Fig.13 show similar tendency. As the  $S_0$  decreases,  $Q_T$  and  $Q_S$  decrease but  $Q_D$  and  $Q_W$  change a little.

3) Effect of rupture extent

Oil spill data are shown in Fig.14 for various rupture extents and their combinations. From these figures,  $Q_T$  and  $Q_S$  change little with the extent of rupture, while  $Q_D$  and  $Q_W$  are seen to change. When the extent of the rupture is large,  $Q_W$  is large but  $Q_D$  is small. If the rupture size of outer hull plating differs from the size of inner hull plating rupture, quantities of both  $Q_D$  and  $Q_W$  are about equal to the quantities for the size of outer hull plating rupture.

4) Effect of rupture position

The data are plotted on Fig.15 to investigate the effect of rupture offset between the hull plating.  $Q_T$ ,  $Q_S$ ,  $Q_D$  and  $Q_W$  are not varied significantly with offset value of  $0.25D_0$ . Differences of  $Q_T$  and  $Q_S$  for different offset value are apparently due to the difference of  $S_0$ .

5) Effect of double bottom height

Fig.16 show the effect of double bottom height on  $Q_T$ ,  $Q_S$ ,  $Q_D$  and  $Q_W$ .  $Q_T$  increases slightly,  $Q_D$  and  $Q_W$  increase with increasing double bottom height.

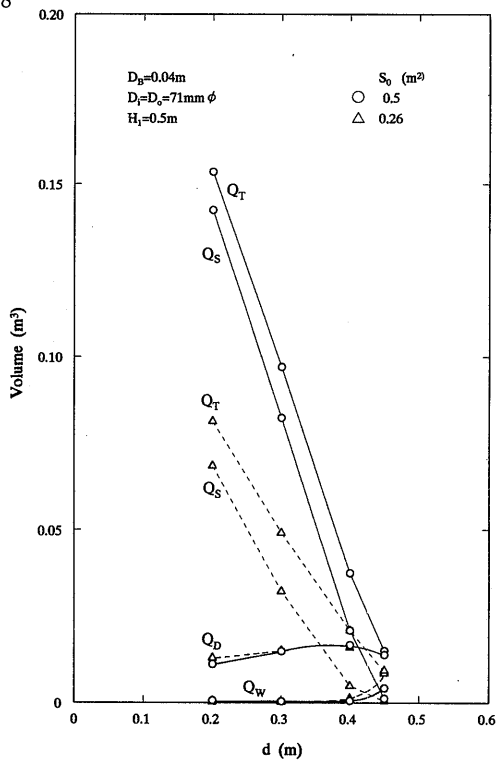


Fig. 13 Effect of cross-sectional area of oil tank on oil spills

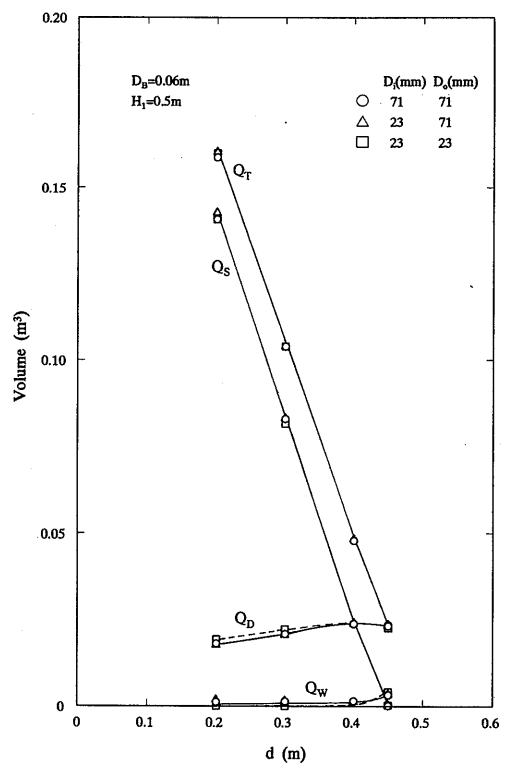
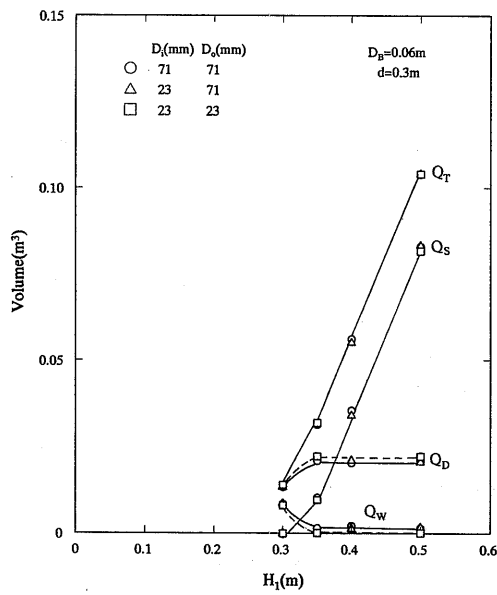
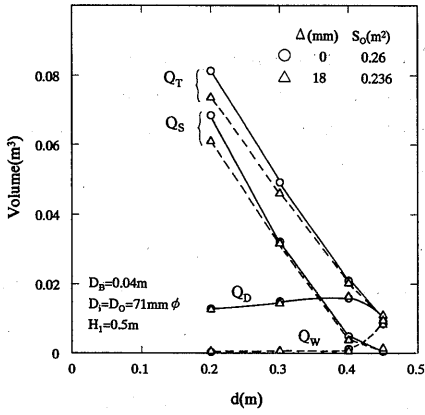


Fig. 14 Effect of puncture diameter on oil spills

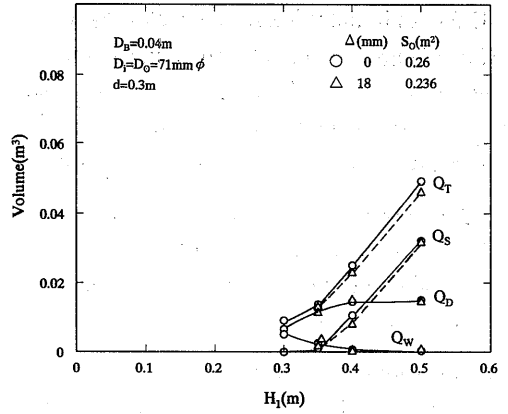


(b)

Fig. 14 Effect of puncture diameter on oil spills

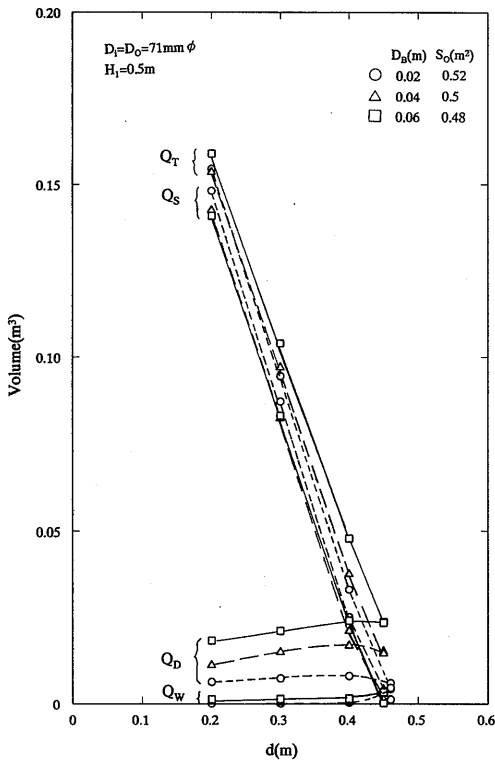


(a)

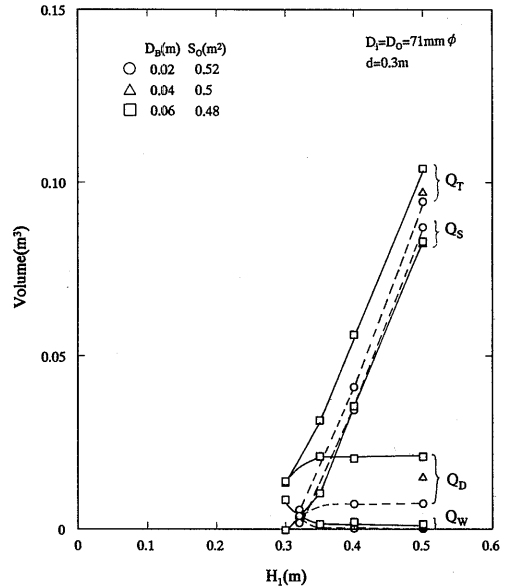


(b)

Fig. 15 Effect of offset value on oil spills



(a)



(b)

Fig. 16 Effect of double bottom height on oil spills

6) Effect of initial thickness of water layer

Fig.17 show the data for the experimental condition that the initial thickness of the water layer is not exceeding the double bottom height. Fig.18 show the data for the case that the initial water level in the double hull is less than the draft. Increasing the initial thickness of the water layer, residual water in the double bottom increases, consequently  $Q_D$  decreases and  $Q_S$  increases.

7.1.2. Side rupture, below water line

Whole oil below the top of the rupture both in oil tank and in double hull spills by replacing with water. Oil above the top of the rupture will remain in the tank. At the puncture, hydrostatic head of oil is equal the head of water.

7.1.3. Side rupture, on water line

Whole oil will be spilled. The cargo oil tank and double hull below water line will be filled with water.

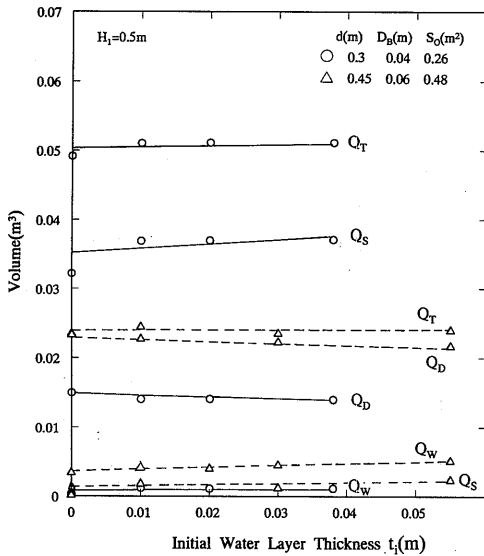


Fig. 17 Effect of initial water layer thickness on oil spills for  $t_i < D_B$

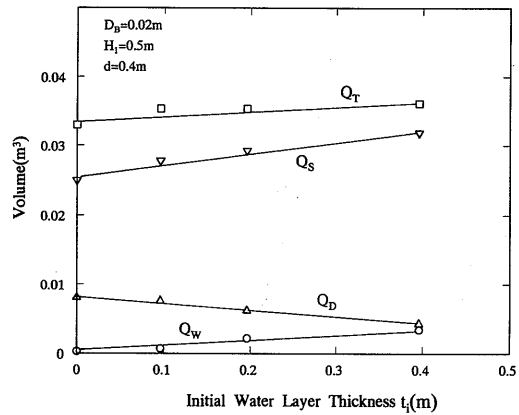


Fig. 18 Effect of initial water layer thickness on oil spills for  $t_i > D_B$

## 8. ANALYSIS OF RESULTS

### 8.1. Oil outflow

On referring to Figure 4, consider oil outflow through the bottom rupture of a tank with double hull begins at oil level  $H_1$  and ceases at oil level  $H$ , oil in cargo tank and surrounding water flow into the double hull during this period. If the quantity of oil spill is  $Q_S$ , oil remained in double hull is  $Q_D$ , and the thickness of the water layer in double bottom is  $t_f$ , then following relations are obtained from the balance of hydrostatic head at the rupture and from the mass balance.

$$\gamma_o H + t_f \gamma_w + (D_B - t_f) \gamma_o = \gamma_w d$$

$$Q_T = Q_D + Q_S$$

Hence, for  $D_S = D_B$

$$Q_S = S_o H_1 - \frac{\gamma_w S_o (d - \alpha D_B)}{\gamma_o} + S_o (1 - \alpha) D_B - Q_D \quad (1)$$

$$Q_D = H D_B \ell + \left( \frac{L_D}{2} + D_B \right) (1 - \alpha) \ell D_B \quad (2)$$

$$Q_T = (H_1 - H) S_o \quad (3)$$

$$Q_W = \alpha D_B \ell \left( D_B + \frac{L_D}{2} \right) \quad (4)$$

$$H = \frac{\gamma_w (d - \alpha D_B)}{\gamma_o} - (1 - \alpha) D_B \quad (5)$$

For a single hull tank, the double bottom height and the double side width are zero, therefore  $\alpha = Q_D = 0$ . In this case Eqs. (1) and (5) become

$$Q_S = S_o (H_1 - H) = S_o H_1 - \frac{\gamma_w S_o d}{\gamma_o} \quad (6)$$

$$H = \frac{\gamma_w d}{\gamma_o} \quad (7)$$

Since  $Q_D$  is obtained from Eq. (2) if the double hull structure is given, the only unknown for  $Q_S$  is the non-dimensional thickness of the water layer  $\alpha$ . In order to examine the sensitivity of the  $Q_S$ ,  $Q_T$ ,  $Q_D$  and  $Q_W$ , we computed from Eqs. (1) to (5) for various parameters ( $L_D = 1.0$  m,  $\ell = 0.45$  m,  $\gamma_w = 1000$  kg/m<sup>3</sup>,  $\gamma_o = 860$  kg/m<sup>3</sup>). They are illustrated in Figs.19 to 23.

It can be seen from these figures that

- oil outflow increases with an increase in  $\alpha$  and
- oil outflow increases with increases in  $D_B$ , cross-sectional area of oil tank and density of cargo oil for constant  $\alpha$  and
- oil outflow from J type double bottom configuration is greater than that from U type one for constant  $\alpha$ .

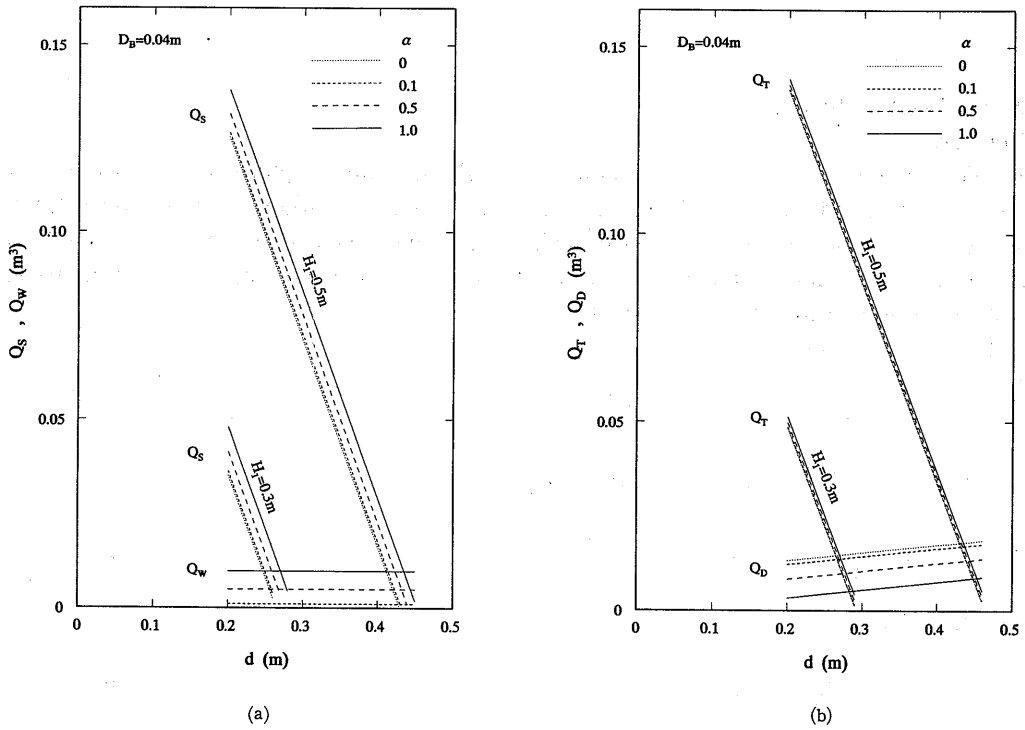


Fig. 19 Values of  $Q_s$ ,  $Q_r$ ,  $Q_d$  and  $Q_w$  as function of  $\alpha$  and  $H_1$  (oil tank-no division, double bottom-J type)

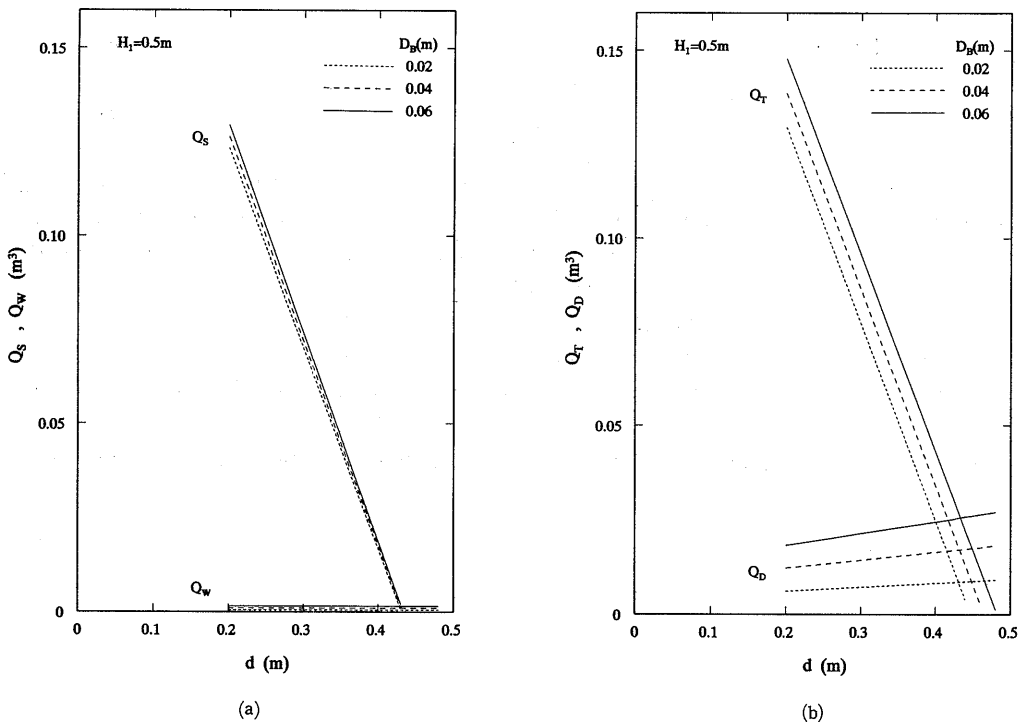


Fig. 20 Values of  $Q_s$ ,  $Q_r$ ,  $Q_d$  and  $Q_w$  as function of  $D_B$  (oil tank-no division, double bottom-J type,  $\alpha=0.1$ )

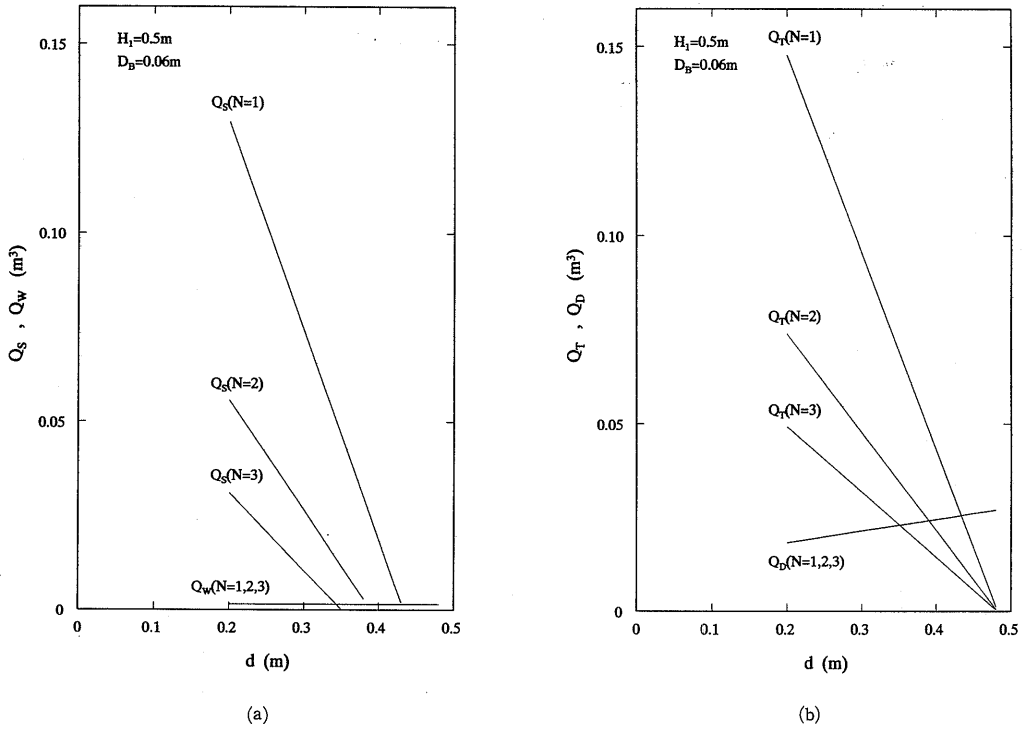


Fig. 21 Values of  $Q_s$ ,  $Q_r$ ,  $Q_d$  and  $Q_w$  as function of oil tank divisions (N: number of divisions, double bottom-J type,  $\alpha=0.1$ )

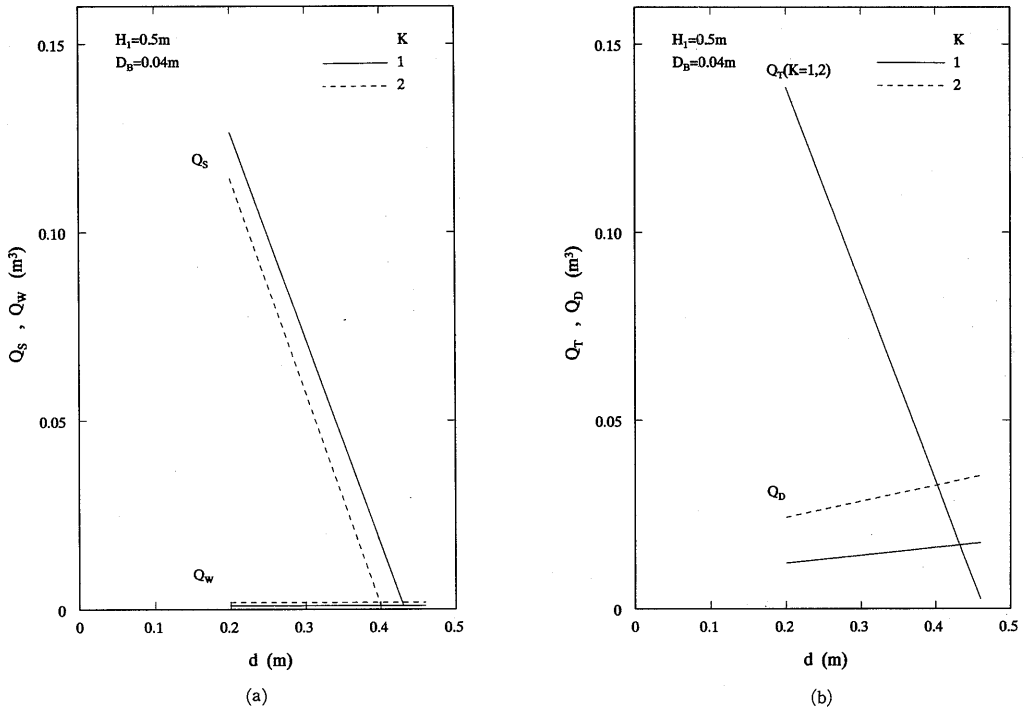


Fig. 22 Values of  $Q_s$ ,  $Q_r$ ,  $Q_d$  and  $Q_w$  as function of double bottom configuration (K=1: J type, K=2: U type, oil tank-no division,  $\alpha=0.1$ )

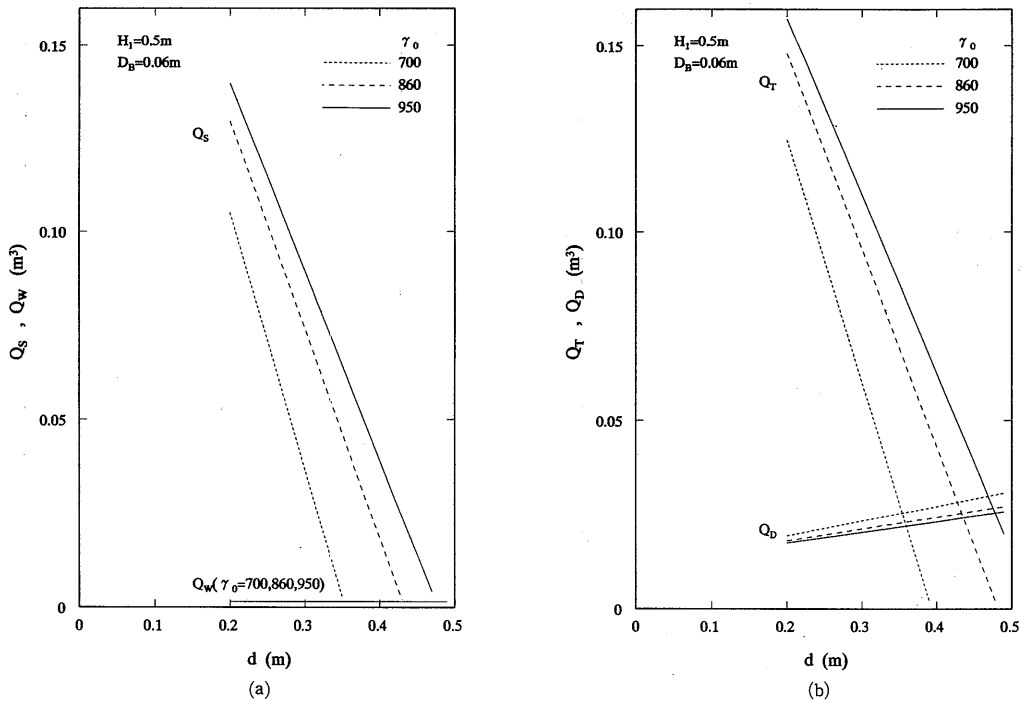


Fig. 23 Values of  $Q_s$ ,  $Q_T$ ,  $Q_D$  and  $Q_w$  as function of cargo oil density (oil tank-no division, double bottom-J type,  $\alpha=0.1$ )

## 8.2. Non-dimensional thickness of water layer $\alpha$

In Fig.24, the experimental results are plotted as the ratio of the water level to the oil level  $d/H_1$  vs.  $\alpha$  with double bottom height as the parameter. Several forms of ratio  $d/H_1$  and  $D_B$  were tried. Same data are plotted on  $\alpha$  vs  $(d-D_B)/H_1$  plane as shown in Fig.25 and on  $\alpha$  vs  $d/(D_B+H_1)$  plane as shown in Fig.26.  $(d-D_B)/H_1$  denotes the ratio of the water level to the oil level at the inner hull rupture,  $d/(D_B+H_1)$  denotes the ratio of the water level to the oil level at the outer hull rupture. By examining and comparing the  $\alpha$  vs  $d/H_1$ ,  $\alpha$  vs  $(d-D_B)/H_1$  and  $\alpha$  vs  $d/(D_B+H_1)$  plane, we note that the  $\alpha$  vs  $d/(D_B+H_1)$  plane represents the data best. The following important characteristics can be drawn from the data plotted on such plane.

- $\alpha$  increases with an increase in  $d/(D_B+H_1)$
- Two distinct regions are found. At low  $d/(D_B+H_1)$ ,  $\alpha$  varies gradually. At higher  $d/(D_B+H_1)$ ,  $\alpha$  varies sharply. In this region, the experimental data show that  $Q_s$  is very small, approximately  $Q_s=0$ .
- The non-dimensional thickness of the water layer  $\alpha$  increases with an increase in double bottom height at low  $d/(D_B+H_1)$ .
- The curves for various double bottom height are seen to merge into one curve, where the effect of the double bottom height disappears.

The effect of  $S_0$  on  $\alpha$  was investigated on Fig.27. Hereinafter, the experimental data correlated by  $d/H_1$  and  $(d-D_B)/H_1$  are presented graphically in Appendix giving the same figure number as the figure that the data are correlated by  $d/(D_B+H_1)$  but adding A.  $S_0$  seems not to affect significantly in low  $d/(D_B+H_1)$  range.



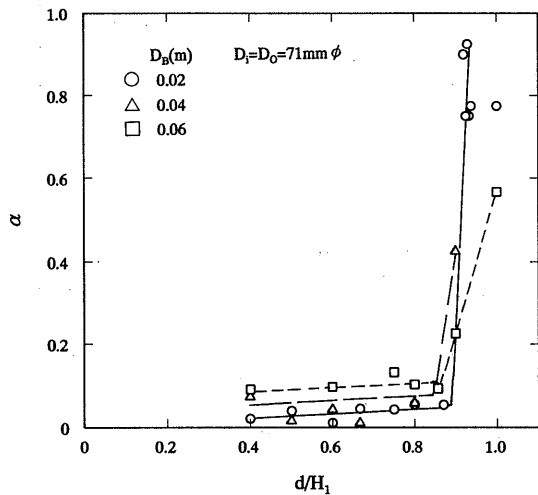


Fig. 24 Effect of double bottom height on  $\alpha$  ( $\alpha$  vs.  $d/H_1$ )

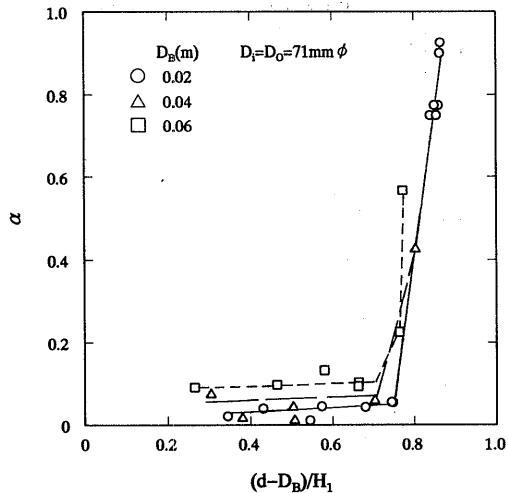


Fig. 25 Effect of double bottom height on  $\alpha$  ( $\alpha$  vs.  $(d - D_B)/H_1$ )

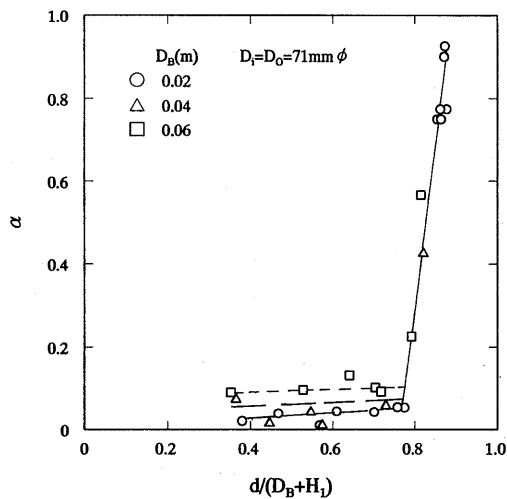


Fig. 26 Effect of double bottom height on  $\alpha$  ( $\alpha$  vs.  $d/(D_B + H_1)$ )

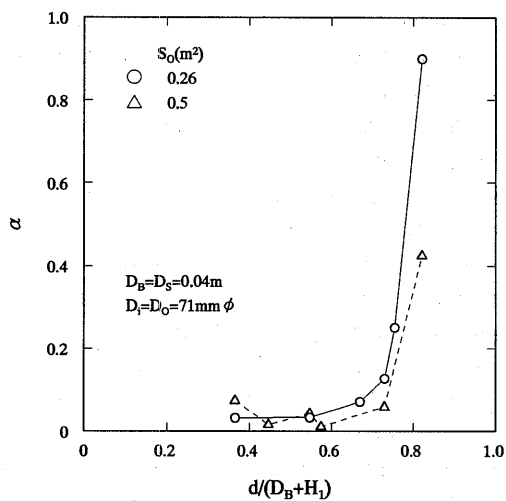


Fig. 27 Effect of  $S_0$  on  $\alpha$

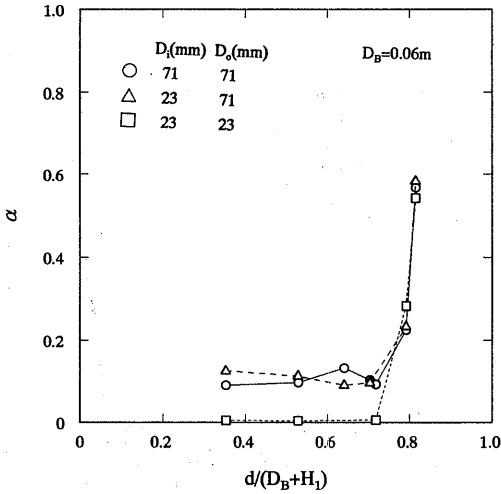


Fig. 28 Effect of rupture diameter on  $\alpha$

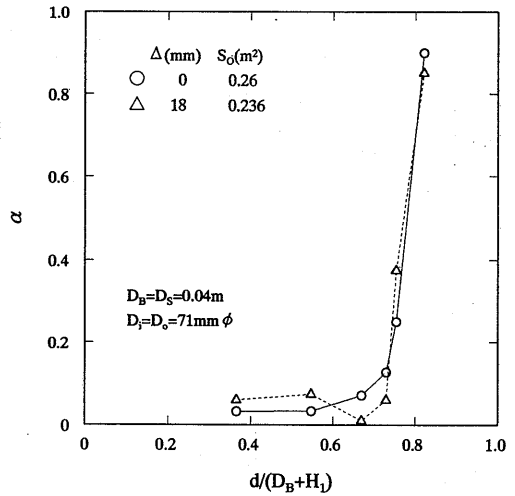


Fig. 29 Effect of  $\Delta$  on  $\alpha$

In Fig.28, the diameter of the rupture has an effect on the value of  $\alpha$  in low  $d/(D_B+H_1)$ ,  $\alpha$  increases with an increase in diameter. Whereas in higher  $d/(D_B+H_1)$ ,  $\alpha$  is not affected by the diameter. If the rupture diameter of outer hull plating is larger than the diameter of inner hull plating,  $\alpha$  is about equal to the value of diameter combination of large-large.

In Fig.29, experimental data have been plotted for the cases when the offset values,  $\Delta$ , of  $0.25D_0$  and  $0$ . It can be seen that the value of  $\alpha$  is not affected very much by offset value.

In groundings which result in the rupture of the inner hull plating after the damage of the outer hull plating has occurred, the double hull space will be flooded by surrounding water before the oil will be spilled.  $\alpha$  are plotted against initial water thickness  $t_i$  for various experimental conditions in Fig.30. As we can see from the figures,  $\alpha$  increases with an increase in  $t_i$ .

As described above, since  $\alpha$  is only function of both the double bottom height and the rupture diameter at low  $d/(D_B+H_1)$ , data are correlated in terms of these variables in Fig.31 for  $t_i=0$ , plotting an average value and range of scatter. It can be seen from Fig.31 that the data show a linear relation with respect to the double bottom height. The slopes of the lines increase with an increase in the rupture diameter. It appears that the ratio of the slope is roughly equal to the ratio of the puncture area. At higher  $d/(D_B+H_1)$ ,  $\alpha$  is only function of  $d/(D_B+H_1)$  and  $S_0$ , and not dependent on the double bottom height, the puncture diameter and the offset value of the puncture as shown in Figs.26 to 29. Inserting these values of  $\alpha$  into Eqs. (1), (2) and (5) they approximately give the quantities of oil outflow.

From Eqs. (1), (2) and (5), diminishing  $Q_D$  and  $H$ ,

$$\alpha = \frac{Q_S - S_0(D_B + H_1) + \gamma_w d(S_0 + D_B \ell) / \gamma_o + 0.5L_D D_B \ell}{-S_0 D_B + \gamma_w D_B(S_0 + D_B \ell) / \gamma_o + 0.5L_D D_B \ell} \tag{8}$$

For  $Q_s=0$ ,  $\alpha$  is calculated from Eq. (8) and compared with the data at higher  $d/(D_B+H_1)$  shown in Figs.26 to 29. Good agreement with experimental data are shown in Fig.32. This fact suggests that value of  $\alpha$  at higher  $d/(D_B+H_1)$  is determined from the hydrostatic head balance between oil and water at the rupture for the condition of  $Q_s=0$ .

### 8. 3. Quantity of oil contained in double hull space

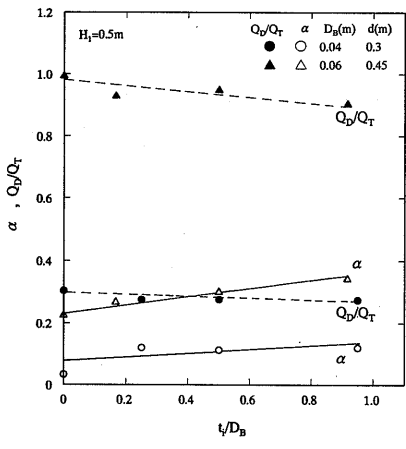
In Figs.30 and 33 to 37 are plotted the experimental data of  $Q_D/Q_T$ . It can be seen that  $Q_D/Q_T$ , denoting the ratio of oil containment in double hull to oil outflow from cargo oil tank, increases with an increase in  $d/(D_B+H_1)$ ,  $(d-D_B)/H_1$ , or  $d/H_1$  for various double bottom heights.

As  $D_B$  increases the value of  $Q_D/Q_T$  increases, resulting in oil spill reduction. On the contrary, as  $S_0$  and  $t_i$  decrease  $Q_D/Q_T$  increases. It may be noted that the values of the ordinate in these figures are zero for single hull tank because  $Q_D$  is zero for all values of the abscissa. It appears, therefore, that the deviation from the axis of abscissa will denote the measure of effectiveness for the double hull tank from the point of view of prevention of oil spills. In Figs.37 to 41, data are plotted as  $Q_D/(Q_D+Q_W)$  vs.  $d/H_1$ ,  $Q_D/(Q_D+Q_W)$  vs.  $(d-D_B)/H_1$ , or  $Q_D/(Q_D+Q_W)$  vs.  $d/(D_B+H_1)$ . As we can see,  $Q_D/(Q_D+Q_W)$  increase with decrease in  $d/H_1$  or  $d/(D_B+H_1)$ .

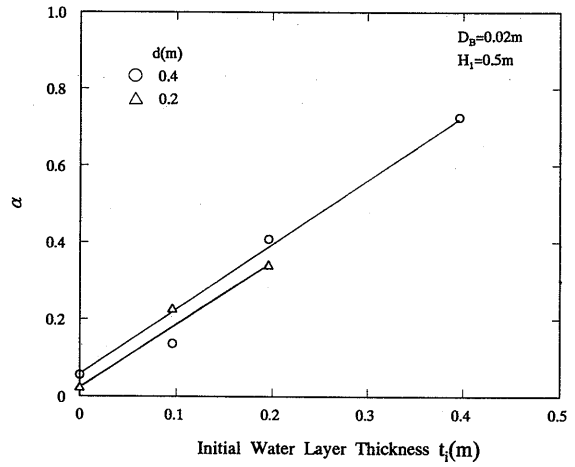
### 8.4. Oil spill fraction

In Figs.42 to 46 are plotted  $\eta_s$ , the ratio of  $Q_s$  to volume of loaded cargo oil  $H_1S_0$ , and  $\eta_T$ , the ratio of  $Q_T$  to  $H_1S_0$ , against  $d/H_1$ ,  $(d-D_B)/H_1$ , or  $d/(D_B+H_1)$  together with the results predicted by Eq. (6) for single hull tank. Generally,  $\eta$  decreases with an increase in  $d/H_1$  or  $d/(D_B+H_1)$ . It can be seen that the variation of  $\eta_T$  for every parameters except  $D_B$  is small.  $\eta_s$  is insignificantly depend on rupture diameter and  $\Delta$  but  $\eta_s$  is significantly affected by  $D_B$ ,  $S_0$  and  $t_i$ .

Since a difference between  $\eta_T$  and  $\eta_s$  is equivalent to non-dimensional oil containment in double hull space, it can be seen that the ruptured double hull tank shows a remarkable effect on oil containment as the  $D_B$  and  $D_s$  increase, and  $S_0$ , the rupture diameter and the initial thickness of the water layer decrease.



(a)



(b)

Fig. 30 Effect of  $t_i$  on  $\alpha$  and  $Q_p/Q_T$

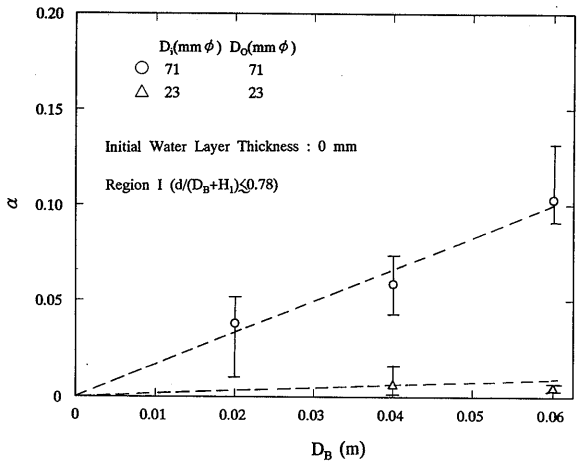
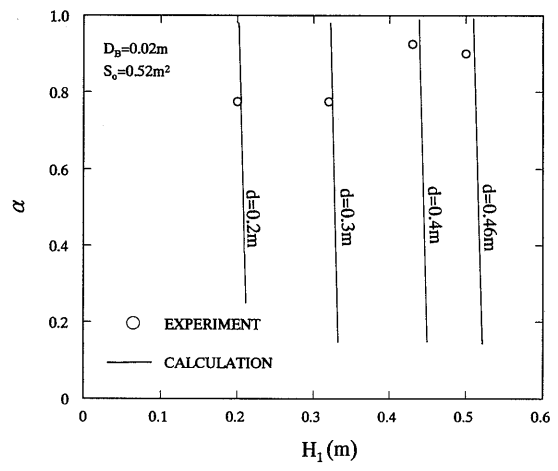


Fig. 31 The value of  $\alpha$  in low  $d/(D_b+H_i)$



(a)

Fig. 32 The value of  $\alpha$  in high  $d/(D_b+H_i)$  comparing with prediction

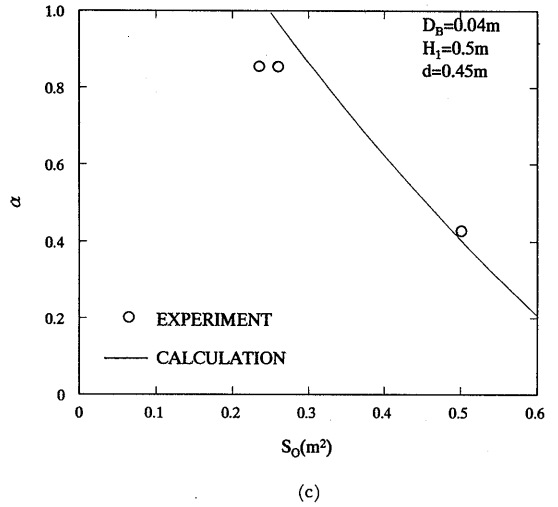
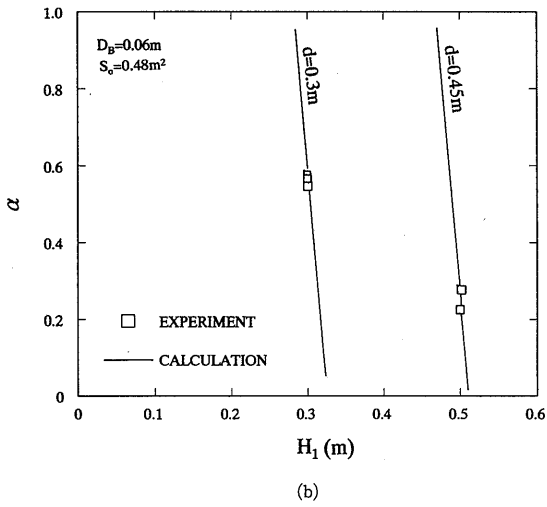


Fig. 32 The value of  $\alpha$  in high  $d/(D_B+H_1)$  comparing with prediction

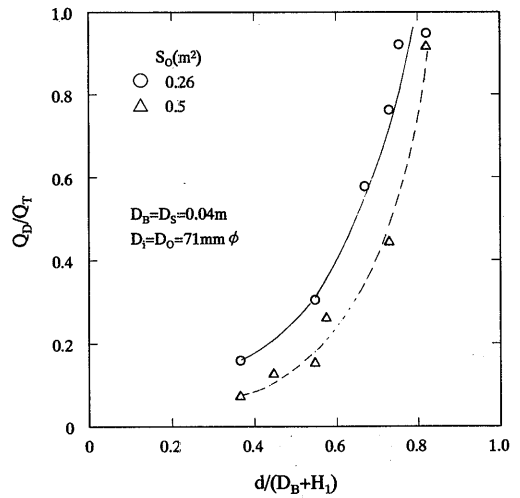
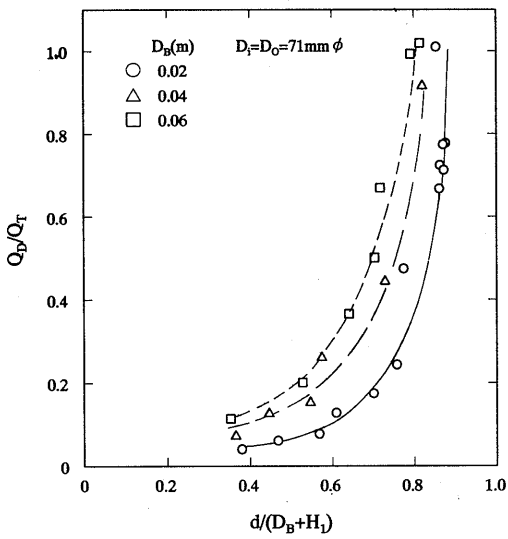


Fig. 33 Effect of double bottom height on  $Q_D/Q_T$

Fig. 34 Effect of  $S_0$  on  $Q_D/Q_T$

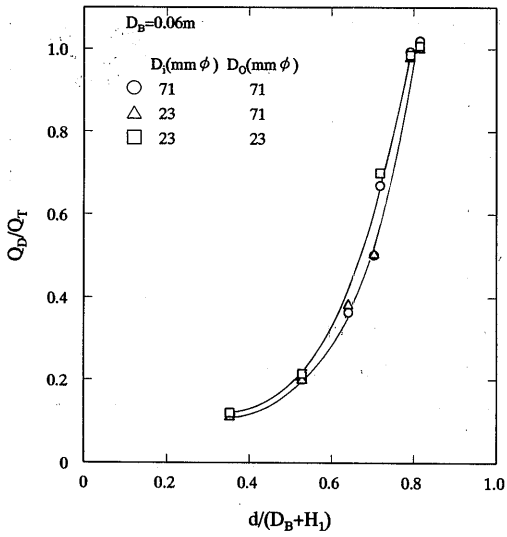


Fig. 35 Effect of rupture diameter on  $Q_D/Q_T$

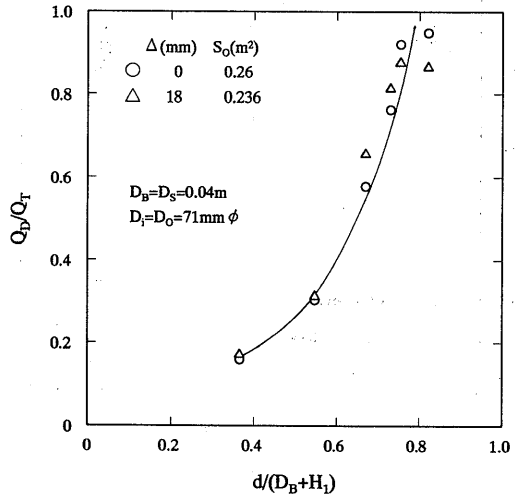


Fig. 36 Effect of  $\Delta$  on  $Q_D/Q_T$

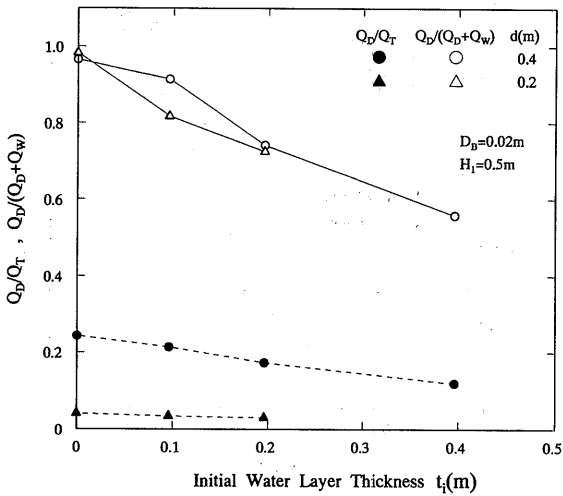


Fig. 37 Effects of  $t_i$  on  $Q_D/Q_T$  and  $Q_D/(Q_D+Q_W)$

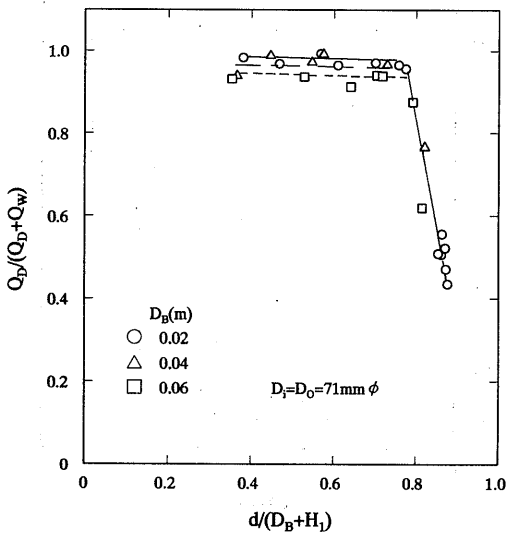


Fig. 38 Effect of  $D_B$  on  $Q_D/(Q_D+Q_W)$

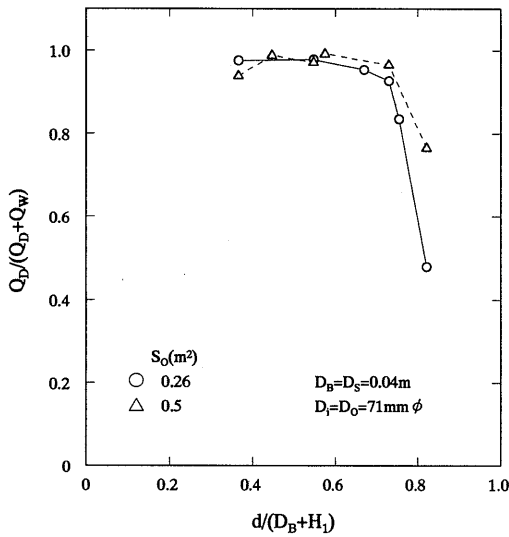


Fig. 39 Effect of  $S_o$  on  $Q_D / (Q_D + Q_W)$

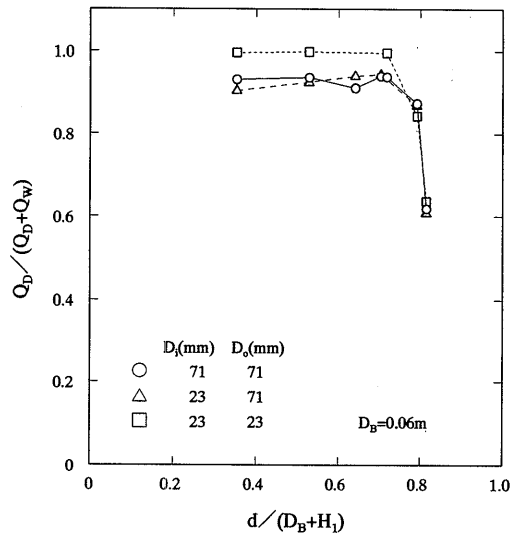


Fig. 40 Effect of rupture diameter on  $Q_D / (Q_D + Q_W)$

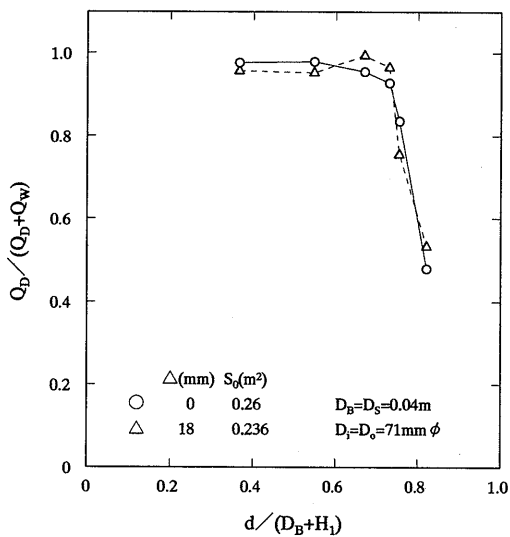


Fig. 41 Effect of  $\Delta$  on  $Q_D / (Q_D + Q_W)$

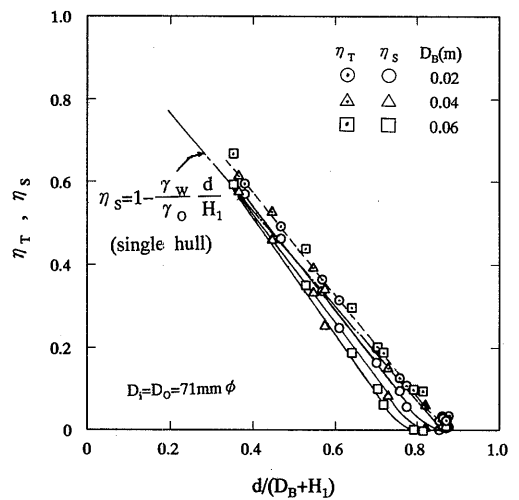


Fig. 42 Effect of  $D_B$  on  $\eta$

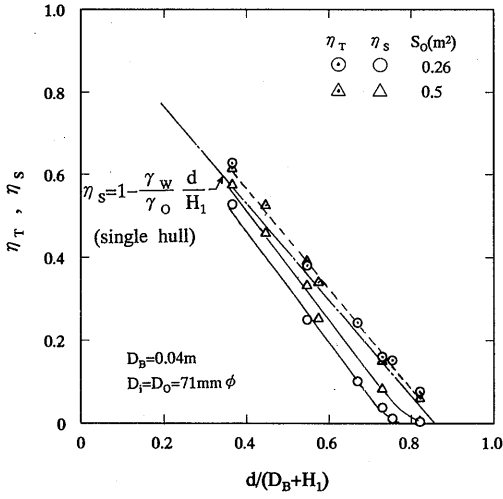


Fig. 43 Effect of  $S_0$  on  $\eta$

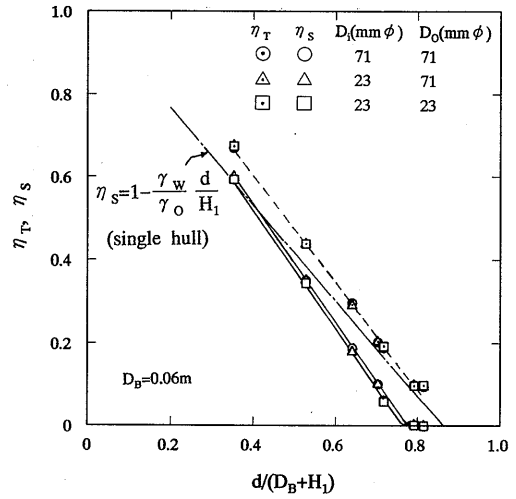


Fig. 44 Effect of rupture diameter on  $\eta$

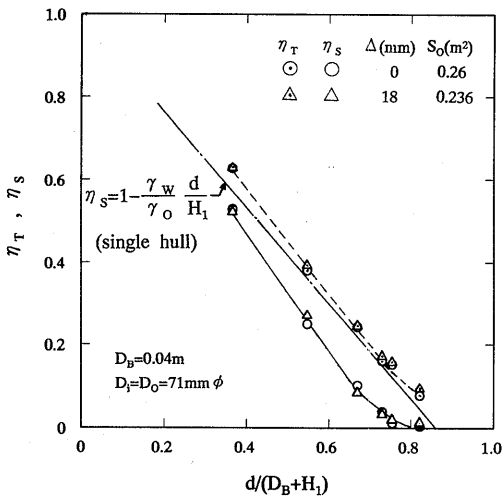


Fig. 45 Effect of  $\Delta$  on  $\eta$

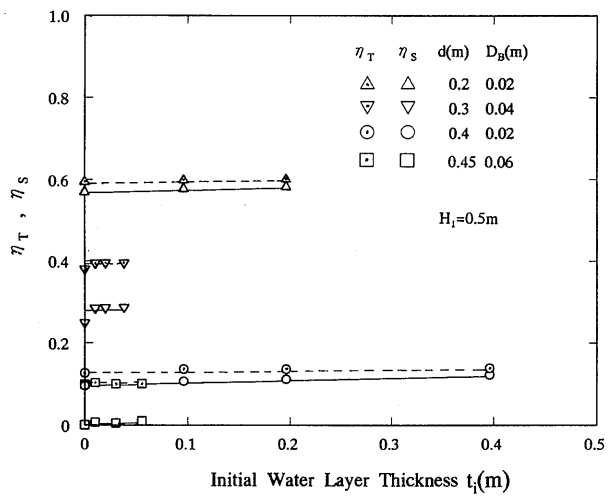


Fig. 46 Effect of  $t_i$  on  $\eta$



## 9. CONCLUSIONS

Oil spills and oil-water mixing were investigated by using ruptured ship tank model with double hull for various accident scenarios, tank configurations and cargo loading conditions. The effects of various parameters on oil spills were found. Methods for predicting the oil spills and for interpreting experimental results are presented.

The principal conclusions are as follow.

For groundings:

- (1) Oil spills decrease with a decrease in the difference of oil and water levels.
- (2) Oil containment in double hull space increases remarkably with an increase in double hull space and with a decrease in cross-sectional area of cargo oil tank, resulting decrease in oil spills.
- (3) Oil spills can be predicted by introducing the non-dimensional thickness of water layer  $\alpha$ .
- (4)  $\alpha$  is a function of tank configuration, tank dimension, rupture area and liquid level.

For collisions:

- (1) All amount of oil below the rupture spills.

Further experimental work is required to study the variation of  $\alpha$  with actual accident data or the full-scale test for the grounding accidents.

## NOMENCLATURE

$A_0$ :	area of rupture
$D_i$ :	diameter of inner hull plating rupture
$d$ :	draft
$D_o$ :	diameter of outer hull plating rupture
$D_B$ :	double bottom height
$D_S$ :	double side width
$H$ :	height of oil level after oil spills
$H_1$ :	initial height of oil level
$K$ :	parameter denoting the configuration of the double bottom K=1; J type, K=2; U type
$l$ :	longitudinal length of oil tank
$L_D$ :	oil tank breadth
$N$ :	number of division of oil tank
$Q_T$ :	quantity of oil leaving from oil tank
$Q_W$ :	quantity of water flows into double hull space
$S_0$ :	cross-sectional area of oil tank
$t_f$ :	thickness of water layer in double hull after oil spills
$t_i$ :	initial thickness of water layer in double hull
$V_O$ :	volume of oil tank
$V_D$ :	volume of double hull space
$\alpha$ :	non-dimensional thickness of water layer ( $= t_f/D_B$ )
$\gamma_o$ :	density of oil
$\gamma_w$ :	density of water
$\Delta$ :	offset value of inner and outer shell plating rupture
$\eta_S$ :	oil spill fraction ( $= Q_S/H_1 S_0$ )
$\eta_T$ :	oil leaving fraction ( $= Q_T/H_1 S_0$ )

ACKNOWLEDGEMENTS

A part of this work was performed as the research program of the Shipbuilding Research Association of Japan. The authors express their appreciation to Prof. H. Otsubo, chief of the committee, and to the other committee members of SRA RR761 for helpful discussions. The authors also are grateful for the encouragement of the head of the Ship Equipment and Marine Environment Division, Ship Research Institute, Dr. O. Nagata.

APPENDIX

Graphical presentation of the experimental data correlated by  $d/H_1$  and  $(d-D_B)/H_1$

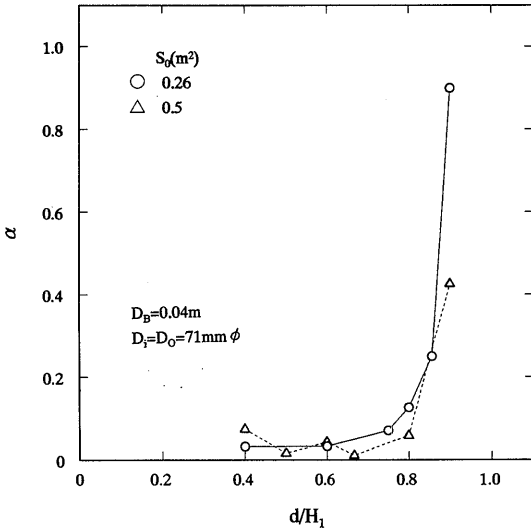


Fig. 27A

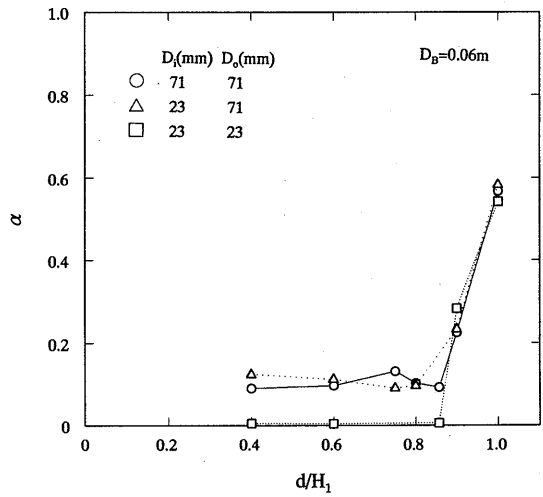


Fig. 28A

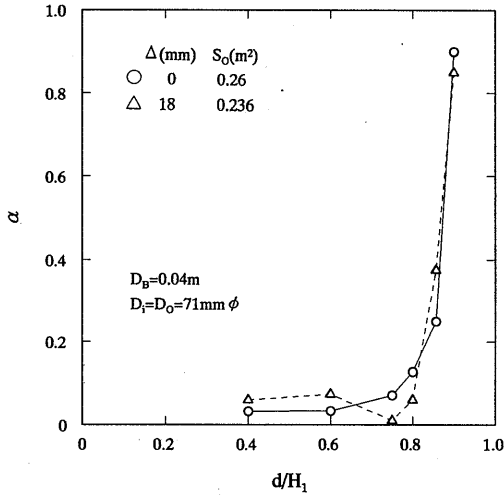
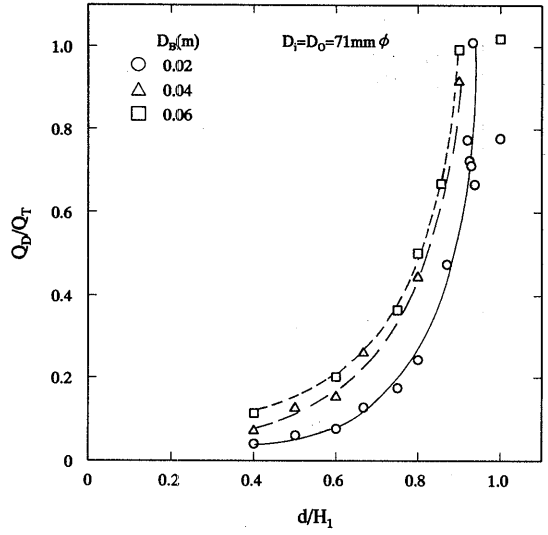
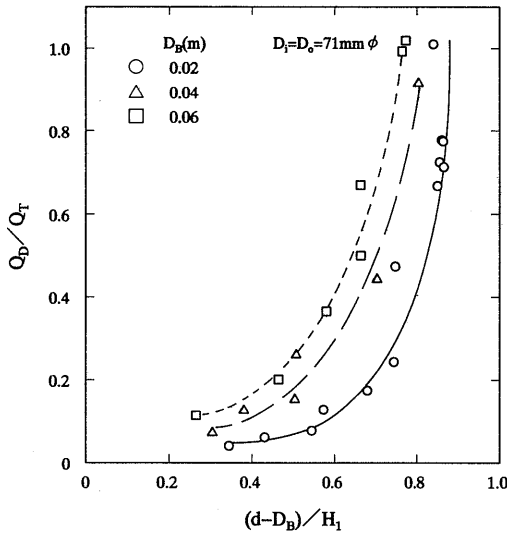


Fig. 29A



(a)  
Fig. 33A



(b)  
Fig. 33A

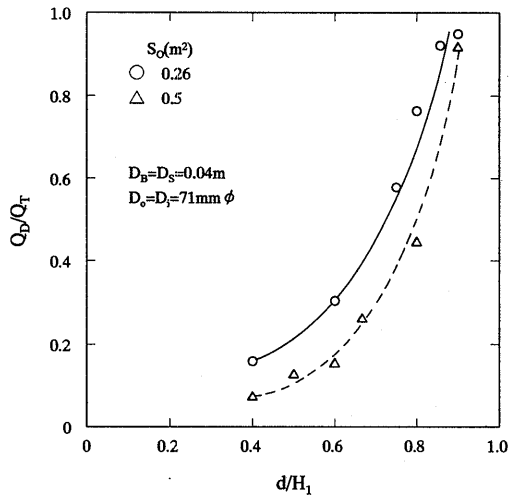


Fig. 34A

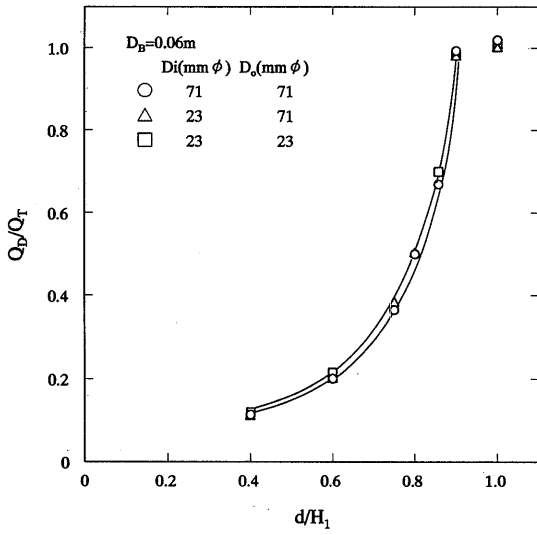


Fig. 35A

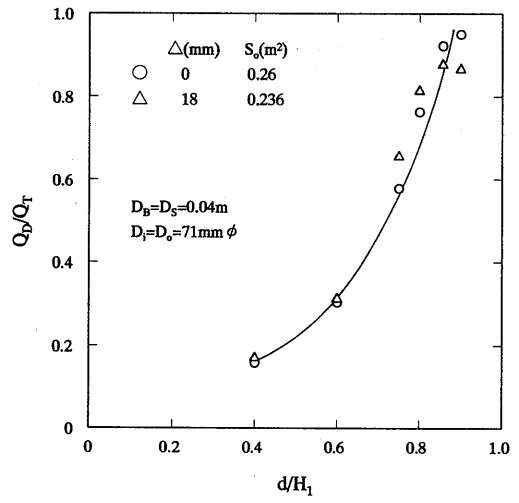
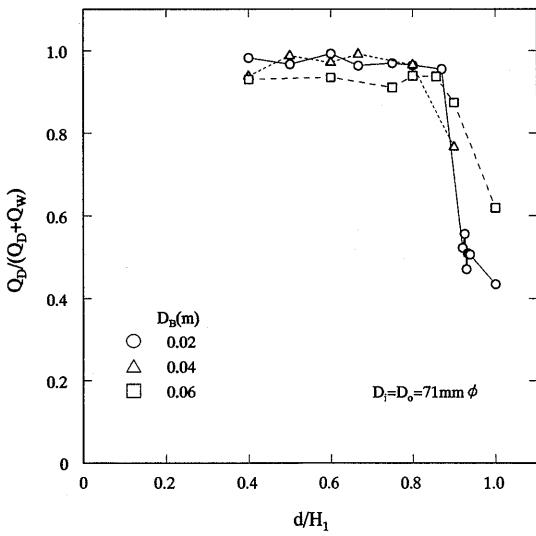
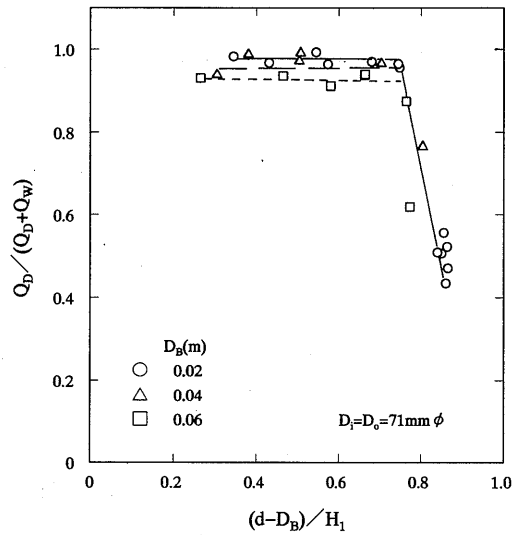


Fig. 36A



(a)



(b)

Fig. 38A

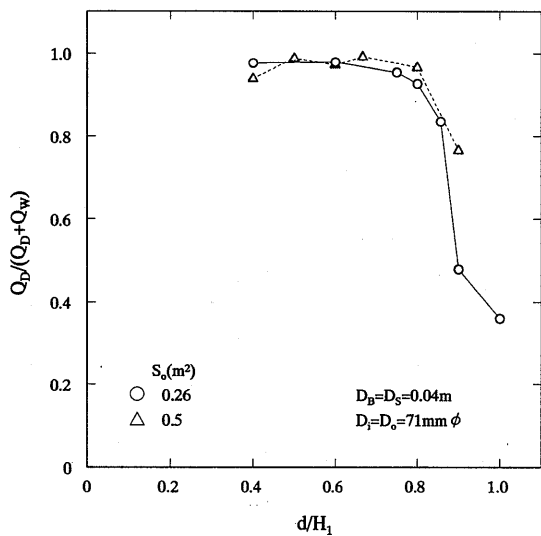


Fig. 39A

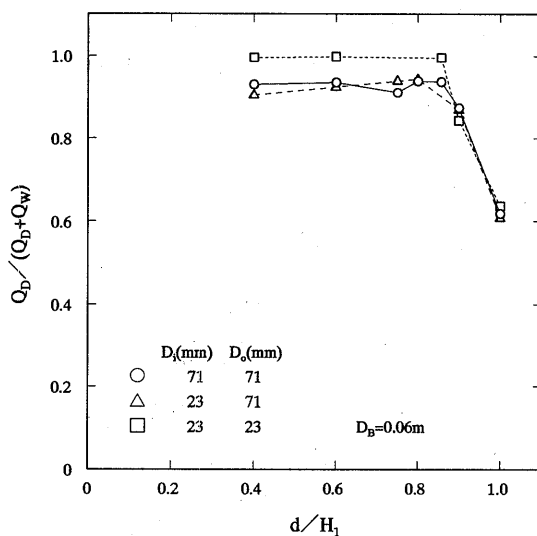


Fig. 40A

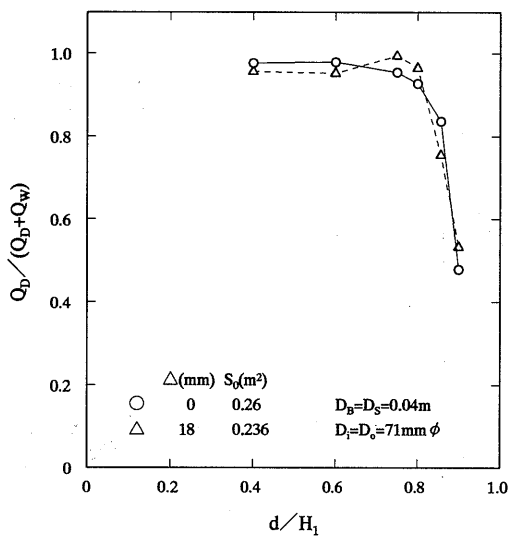
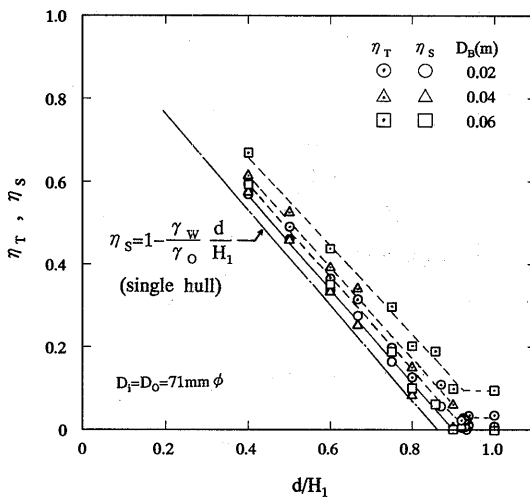
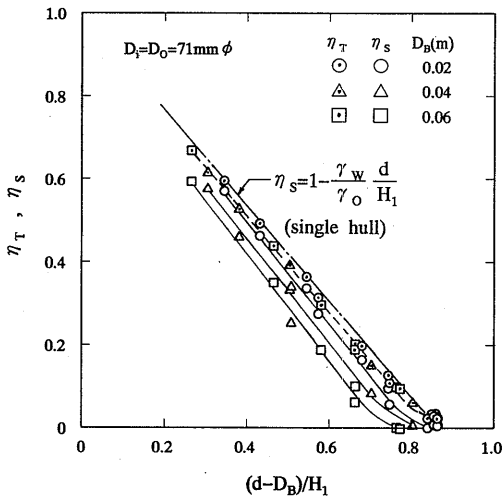


Fig. 41A



(a)  
Fig. 42A



(b)  
Fig. 42A

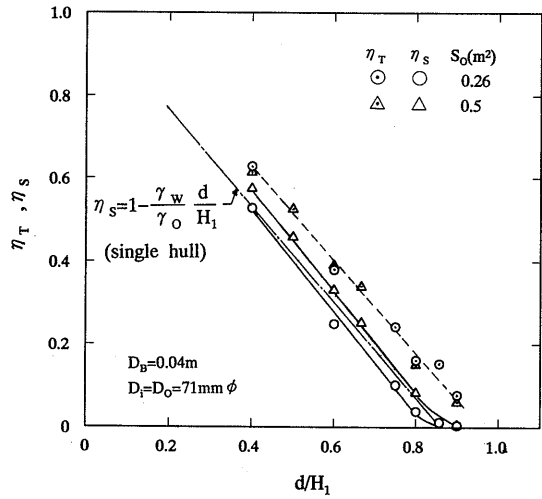


Fig. 43A

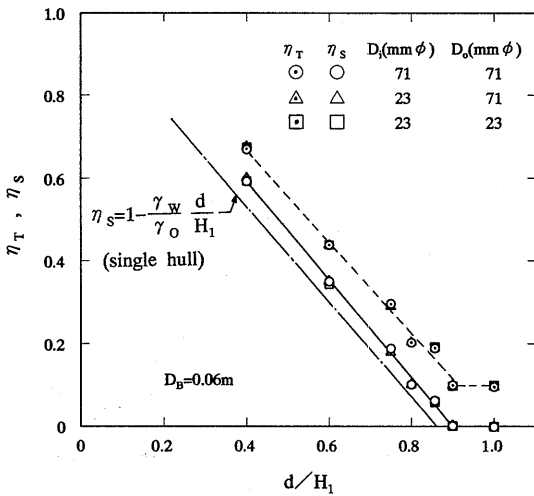


Fig. 44A

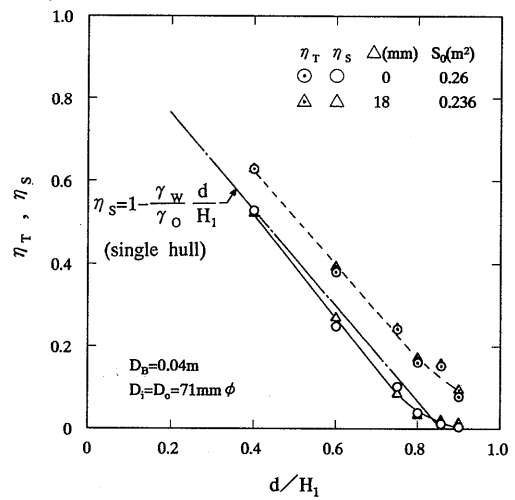


Fig. 45A